Online Temperature Monitoring And Control Of Wire Arc Additive Manufacturing

M.Tech. Thesis

by

Manish Patidar

DISCIPLINE OF MECHANICAL ENGINEERING

INDIAN INSTITUTE OF TECHNOLOGY INDORE

June 2020

Online Temperature Monitoring And Control Of Wire Arc Additive Manufacturing

A THESIS

Submitted in partial fulfillment of the requirements for the award of the degree
of
Master of Technology
in
Mechanical Engineering
with specialization in
Production and Industrial Engineering
by

Manish Patidar

DISCIPLINE OF MECHANICAL ENGINEERING

INDIAN INSTITUTE OF TECHNOLOGY INDORE

June 2020

INDIAN INSTITUTE OF TECHNOLOGY INDORE

CANDIDATE'S DECLARATION

I hereby certify that the work which is being presented in the thesis entitled **Online Temperature Monitoring And Control Of Wire Arc Additive Manufacturing** in the partial fulfillment of the requirements for the award of the degree of **MASTER OF TECHNOLOGY** and submitted in the **DISCIPLINE OF MECHANICAL ENGINEERING, Indian Institute of Technology Indore**, is an authentic record of my own work carried out during the time period from May 2019 to June 2020 under the supervision of **Dr. Yuvraj K Madhukar,** Discipline of Mechanical Engineering, Indian Institute of Technology Indore.

The matter presented in this thesis has not been submitted by me for the award of any other degree of this or any other institute.

Manish Patidar
(1802103003)

16-06-2020

This is to certify that the above statement made by the candidate is correct to the best of my/our knowledge.

19/06/2020

Dr. Yuvraj K Madhukar

Manish Patidar has successfully given his M.Tech. Oral Examination held on 22-06-2020

Signature of the Thesis Supervisor Dr Yuvraj K Madhukar Date: 22/06/2020	Signature of Convener, DPGC Date:
Signature of PSPC Member 1 Dr. Satyajit Chatterjee Date: 22/06/2020	Signature of PSPC Member 2 Dr. Santosh Hosmani Date: 22/06/2020

ACKNOWLEDGEMENT

I take this opportunity to express my deep sense of respect and gratitude for, Dr Yuvraj Kumar Madhukar, for believing in me to carry out this work under his supervision. His constant encouragement, friendly interactions, and constructive support have enabled this work to achieve its present form. His innovative perspective towards things and his continuous pursuit for perfection has had a profound effect on me and has transformed me majorly. He has been provided helpful career advice and suggestions, extending beyond academic boundaries, whenever needed. I feel privileged to be one of his students.

I want to take this opportunity to thank my PSPC members Dr Satyajit Chatterjee and Dr Santosh S. Hosmani, for their valuable suggestions in assessing my work during the mid-term and end-term presentations.

I express my sincere gratitude to PhD Scholar Mr Anas Ullah Khan and B.Tech students Saurav Kumar and Saurabh Kumar for their initial technical assistance to my project. Their involvement in the work from the first day I joined the last is highly acknowledged. I would also like to express my thanks to Mr Anand Petare, DGM, Central Workshop and all the staff of Central Workshop, IIT Indore, especially Mr Rishiraj Chouhan, for extended help.

I express my sincere thanks to Dr Satyajit Chatterjee, for allowing to access the Metallography and Tribology Laboratory facilities. The Discipline of Mechanical Engineering, IIT Indore, is gratefully acknowledged for giving me an opportunity to carry out my M.Tech and needed thesis research work.

A heartfelt thanks to my entire M.Tech 2018 Batch, with whom I have spent most of my time at IIT Indore; especially, Aakanksha Chaudhary, Abhay Tiwari, Ankit Kumar, Akshay Jain, Balaji K Nanda, Akshay D Mate, Eklavya Tripathi, Farhan Ali, Garima Gupta, Jaideep Singh Jadon, Janmejay Sharma, Manoj Tripathi, Pavan Sahapurkar, Pradyuman Arya, Shadab Ali, Shivam Gupta, Shubham Menkar for being my second family. Thanks are also extended to Shivani Awasthi and Tanvir Kaur from M.Sc 2020 Batch for being good friends.

Lastly, but undoubtedly the most valued, gratitude is expressed for my mother, Kala Patidar, and my father, Suresh Patidar, for receiving my ordinary feats in an ever extraordinary way and letting me be the chooser of my own destiny.

Manish Patidar

Dedicated

To

My Family

And

My Friends

ABSTRACT

Additive manufacturing (AM) is the process of joining materials to make parts or objects from 3D model data, usually layer upon layer, as opposed to subtractive manufacturing methodologies. The Direct Energy Deposition (DED) is a series of several similar AM technologies that creates parts by melting and fusion process. The combination of an electric arc as heat source and wire as feedstock is referred to as wire arc additive manufacturing (WAAM). The WAAM uses gas metal arc welding (GMAW), gas tungsten arc welding (GTAW) and plasma arc welding (PAW) as a source for deposition. The GTAW or tungsten inert gas (TIG) welding is used in many applications such as surface hardening, melting, alloying, cladding, additive manufacturing, and many others despite its primary application of quality welding. The mechanical and geometrical properties of the product manufactured by the process are mainly dependent on the thermal characteristics. In this experimental study, in-situ monitoring and control of the generated temperature are proposed to obtain the desired properties. The proposed model consists of three parts, namely instrumental control, in-situ monitoring of temperature and its feedback control in LabVIEW-PID. The fast, error-free and emissivity independent temperature monitoring was complemented with the help of a ratio pyrometer. The primary constraint, i.e. the automation of the process was achieved by replacing the foot pedal of the TIG power source with an in-house developed control system consisting of a data acquisition (DAQ) system and relays. The TIG current was made variable automatically based on the desired or set point temperature. A wide range of experiments was performed to establish the process capability such as constant and dynamic temperature control, on the substrate with a stationary and moving heat source (TIG torch). The feedback temperature control was achieved successfully for the range of temperature between 400°C to 1600°C. A single bead was also deposited with a controlled temperature between 1200°C to 1400°C at different deposition speeds. It was observed that by controlling the bead deposition temperature, its geometrical properties could be altered which would eventually determines the mechanical property. The optimised PID constants were found to be 1.0, 0.04 - 0.08, and 0.0 for proportional, integral and derivative, respectively. The error in controlled temperature was found in between 0.3–1.67% (5-25°C) for different sets of the experiments, where the maximum error was realised for the dynamic and bead deposition temperature control 1–1.67% (15-25°C). It was observed that the stabilisation time for attaining the setpoint temperature was dependent on the nature of the heating source, i.e. stationary or moving. In the case of the stationary heat source, the time taken for controlling the temperature was lesser as compared to the moving heat source where the temperature changes rapidly.

LIST OF PUBLICATION

- **Manish Patidar**, Anas Ullah Khan, Yuvraj K Madhukar, "Finding the Emissivity of Tungsten Using Ratio Pyrometer", International conference on precision, Meso, Micro &Nano Engineering, COPEN-11, IIT Indore, India, 12^{th} – 14^{th} December 2019.

- A U Khan, **M Patidar**, A C Petare, R Chouhan, P Chouhan, B Vishwakarma, U Sharma, S Kaushal, D Dhepte, Y K Madhukar*, "Development of Barrel Finishing Machine to Improve Surface Finish of the Wire Arc Additive Manufactured Parts", 30^{th} CIRP Design Conference, Tshwane University of Technology (TUT), Republic of South Africa ,5^{th}–8^{th} May 2020.

TABLE OF CONTENTS

TABLE OF FIGURES

ABBREVIATION

AM	Additive Manufacturing
AO	Analog output
ASCII	American Standard Code for Information Interchange
CAD	Computer-Aided Design
CNC	Computer Numeric Control
DAQ	Data Acquisition
DCED	Direct Current Electrode Negative
DED	Direct Energy Deposition
DO	Digital Output
GTAW	Gas Tungsten Arc Welding
GMAW	Gas Metal Arc Welding
HF	High Frequency
IR	Infrared Radiation
LabVIEW	Laboratory Virtual Instrument Engineering Workbench
ND	Neutral Density
OD	Optical Density
PAW	Plasma Arc Welding
PID	Proportional Integral Derivative
SOD	Stand-Off Distance
TIG	Tungsten Inert Gas
VISA	Virtual Instrument Software Architecture
WAAM	Wire Arc Additive Manufacturing

Chapter 1 Introduction

1.1 Additive Manufacturing

Additive manufacturing (AM) is the process of joining materials to make parts or objects from 3D model data, usually layer upon layer, as opposed to subtractive manufacturing methodologies. The additive manufacturing is also called rapid prototyping, 3D printing etc. It can produce complex geometrical net or near-net shapes and ready to use products. Earlier it was used for fast fabrication of prototypes to check shape, size and functions, as the AM has freedom in part design and also the capability to reduce the production time, waste and cost [1]. Nowadays, additive manufacturing is widely used in automotive, aerospace, biomedical, defence, electronics and construction etc. sectors [2]. Also, the additive manufacturing is expected to be a key technology in the fourth industrial revolution, i.e. industry 4.0 [3].

There are a lot of material deposition techniques which divide into several parts-

- Powder Bed Fusion.
- Material extrusion.
- Vat photopolymerisation.
- Direct Energy Deposition.
- Material jetting.
- Binder jetting.
- Laminated object manufacturing (LOM).

The above discussed AM includes the use of metal and its alloys, ceramics, polymer, composites, fibres, woods etc. the broad range of work material also makes additive manufacturing important.

1.2 Wire Arc Additive Manufacturing (WAAM)

The arc-based additive manufacturing processes are growing fastly in the manufacturing industry as it can fabricate metal components in lower cost with shorter production time [4]. Direct Energy Deposition (DED) is a series of several similar metal 3D printing technologies that creates parts by melting and fusing material as it is deposited. The combination of an electric arc as heat source and wire as feedstock is referred to as wire arc additive manufacturing (WAAM). WAAM consist welding power source, torches and wire feeding systems, as shown in Figure 1. The material is deposited by giving the motion to the torch either by using CNC gantries or by robotic systems. This tool-less method is capable of producing fully dense part in less time.

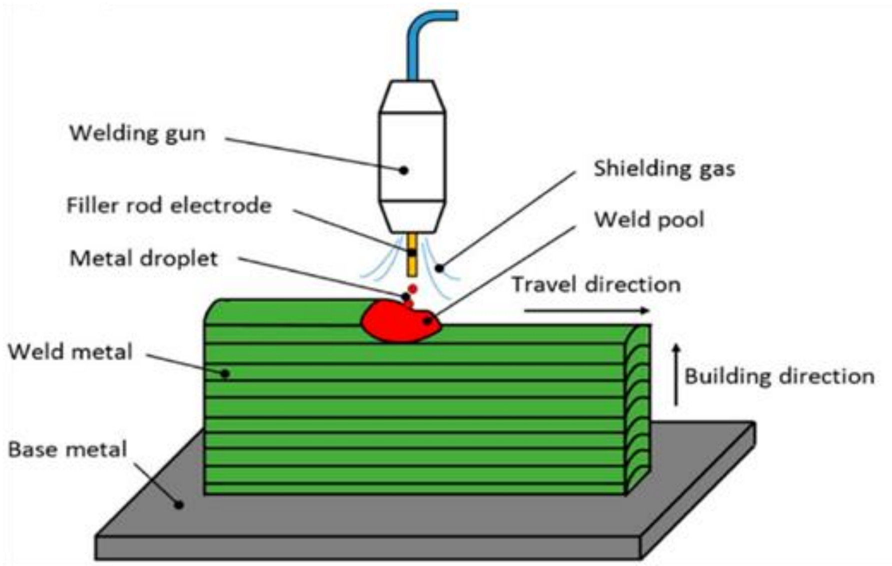

Figure 1: Wire Arc Additive Manufacturing [5]

Although WAAM has many advantages, few reasons are there which limits its applications:

- heating involved in welding processes it induces residual stresses and distortion in manufactured parts [6].
- The fabricated parts relatively poor, When compared with the laser-based process, which requires significant post-processing for application acceptance [7].
- The presence of a large number of voids between deposited layers [8]
- Automation in the field of additive manufacturing is not developed [4].
- The absence of process monitoring and control during deposition limits its application [4].

Generally, the deposition of material in wire + arc additive manufacturing (WAAM) is done with the help of

- Gas metal arc welding (GMAW)
- Gas tungsten arc welding (GTAW)
- Plasma arc welding (PAW)

1.2.1 WAAM parts example

The WAAM deposited bead height is generally 1 to 2 mm. The presence of surface roughness or waviness of bead required further finishing. Due to limited research WAAM is suitable for low to medium complex parts. Also, it has limitations means it is not suitable for small scale parts.

Figure 2a shows 1.2 m wing spar, which was deposited by plasma arc welding.

Figure 2b shows the ship propeller of diameter 1.3 m; it was used in the ship after post-processing.

Figure 2c shows the wing for the wing tunnel testing. It was developed to reduce the testing time as it can be produced in a few hours.

Figure 2d shows the truncated cone with a wall thickness of 2.5 mm. All the above discussed WAAM parts show the capability of the process.

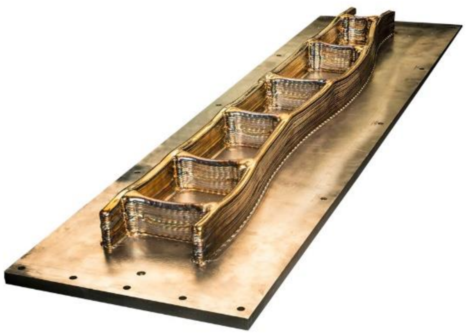

(a)

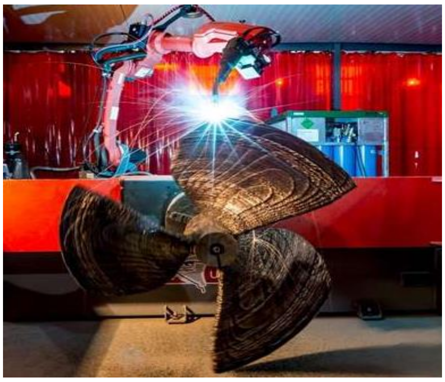

(b)

(c)

(d)

Figure 2: WAAM Parts [12]

1.3 Comparison of various WAAM Techniques [9]

Table 1: WAAM types based on deposition technique and its characteristics

WAAM type	Power source	Characteristics
GTAW-based	GTAW	Non-consumable electrode. Separate wire feed process. deposition rate: 1-2 kg/hour. Wire and torch rotation is needed.
GMAW-based	GMAW	Consumable wire electrode. deposition rate 3-4 kg/hour. Poor arc stability, spatter.
PAW-based	Plasma	Non-consumable electrode. Separate wire feed process. deposition rate 2-4 kg/hour. Wire and torch rotation is needed.

1.4 Gas Tungsten Arc Welding (GTAW)

Gas tungsten arc welding (GTAW), also known as tungsten inert gas welding. It is an arc-based welding process which uses non-consumable tungsten electrode for the generation of arc, as shown in Figure 3. The filler rod is used to fill the gap. The weld bead is protected from oxidation by an inert gas (argon). It is useful in many applications due to its capability to promote all three types of welding, namely autogenous, homogeneous and heterogeneous. Here this autogenous, homogeneous and heterogeneous welding process is referring to the process where no-filler material, the filler similar to the base material, and the filler different from the base material is used, respectively.

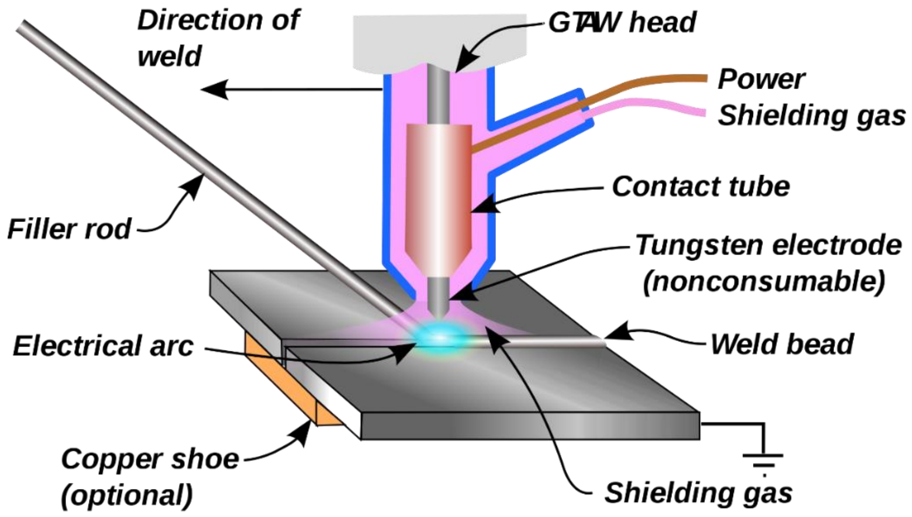

Figure 3: GTAW Schematic [5]

Many researchers have widely studied this welding process for the welding of a broad range of material, including metals and alloys, to explore the various advantages and the process applicability [1–5]. This method produces quality weld in comparison to gas metal arc welding. The plasma arc welding has concentrated energy source and often automated; hence it is faster than GTAW.

1.5 Monitoring Technique

The high complexity and transformations during manufacturing reduce the part quality and repeatability of the process. This challenges can be overcome by monitoring the process variables. The temperature or temperature cycle during deposition is one of the process variables. The uniform temperature during deposition improved mechanical properties. The controlling of the process need errorless monitoring of the temperature [10]. The hazardous environment and arc temperature can damage contact-type measurement devices, so the non-contact type measurement is best suited for these applications.

1.5.1 The Advantages of Non-contact Temperature Measurement:

- The temperature measurement of a moving object is possible.
- The system has a very high response time.
- It can work in a hazardous environment.
- The broad range of temperature measurement is possible.
- Physical interaction avoided hence non-destructive measurement.
- No mechanical damage induced in to test sample.

1.5.2 Infrared Measurement Principle

Each body has a temperature higher than absolute temperature (273.15 °C) emits an electromagnetic radiation from its surface. The part of this electromagnetic radiation ranging from 700 nm to 1 mm, is called infrared radiation (IR), which is used for temperature measurement [10].

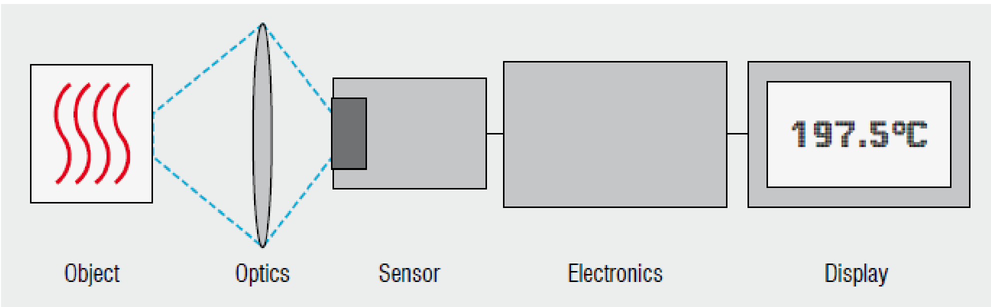

Figure 4: Infrared System [11]

The infrared setup used in pyrometer for temperature measurement is shown in Figure 4. The radiation coming from the object is focused on a detector with the help of suitable optics. The detector generates an electrical signal which is proportional to radiation absorbed. The electrical signal is further processed, and the object temperature is calculated based on the black body radiation principle. The resultant temperature is displayed on a screen, or it can be used as an analog input signal to control some other system [11].

According to Planck's law of black body radiation, the spectral energy density R as a function of wavelength λ (m) and temperature T(K) is given by :

$$R_\lambda\ (T) = \frac{2\pi c^2 h}{\lambda^5} \frac{1}{e^{hc/\lambda kT}-1}$$

Where, c = 3×108 m/s , Speed of light
h = 6.626 × 10-34 J-s, Planck's constant
k = 1.38 × 10-23 J/K, Boltzmann constant

The two types of standard operational mode available in the pyrometer are

1. Single-channel mode.
2. Ratio mode (two colour).

1.5.3 Ratio Mode Pyrometer

Single-channel pyrometer works on a single wavelength band whereas ratio mode works on two adjacent wavelength band. The ratio mode pyrometer has the advantage that a correct measurement of the absolute temperature is possible without knowing the surface emissivity. An error will only arise if the surface emissivities are not equal at the two operating wavelengths of the pyrometer.

It follows that a single measurement of the radiation emitted within a range of wavelengths cannot lead to an unambiguous temperature measurement unless the effective emissivity is practically constant. But if the energy in two narrow wavebands centred at λ_1 and λ_2 is measured, the ratio $R_{12} = \frac{R_{\lambda_1}\ (T)}{R_{\lambda_2}\ (T)}$ becomes Independent of the emissivity provided that $\mathcal{E}_1/\mathcal{E}_2$ is constant. This is the principle of the two-colour pyrometer.

Where,

$$R_{\lambda_1}\ (T) = \frac{2\pi c^2 h}{\lambda^5} \frac{1}{e^{hc/\lambda kT}-1}$$

$$R_{\lambda_2}\ (T) = \frac{2\pi c^2 h}{\lambda^5} \frac{1}{e^{hc/\lambda kT}-1}$$

1.6 Organisation of Thesis

Chapter 2 presents the detailed literature review on the past work reported in the relevant field of wire arc additive manufacturing, tungsten inert gas welding and its automation, monitoring of WAAM, the objectives of research and research methodology used in the present work.

Chapter 3 includes non-contact temperature monitoring and its validation. The different set of experiments were performed to find the effect of external radiation, presence of fumes, dirt and dust in temperature measurement. The experiment was also extended to find the emissivity of the unknown surface. A detailed analysis was performed and discussed in the chapter.

Chapter 4 presents the automation of commercially available non-programmable TIG welding machine and in-situ temperature monitoring. The exhaustive coherent experiments were conducted to establish the feedback control of the generated temperature. The different time-temperature plots show temperature monitoring and controlling of stationary arc, temperature monitoring and controlling of moving arc, temperature monitoring and controlling of moving arc with deposition.

Chapter 5 highlights the conclusions of the present work and marks the scope for future work based on the limitations of the present work.

Chapter 2 Literature Review and objective formulation

This chapter presents the detailed literature review on the past work reported in the relevant field of arc-based additive manufacturing, limitations, usage of TIG based processes, the identified research gaps, the research objectives defined to bridge the identified research gaps and research methodology used in the present work.

2.1 Additive Manufacturing Process (WAAM)

Wu et al. discussed the various aspects of arc-based additive manufacturing (tungsten inert gas welding, gas metal arc welding, plasma arc welding, etc.) including mechanical, structural and microstructural properties. They also addressed that various defects commonly observed in the process such as porosity, residual stresses and cracking, etc. are due to the variation in thermal characteristics during the deposition. They found that the online temperature and heat input can be controlled in a range to get the desired microstructure and mechanical properties. Further, the changing in arc parameters and metal transfer at the same time makes the process stable and defect-free [9].

Williams et al. reported that the wire arc additive manufacturing (WAAM) process could replace current manufacturing trends where blooms and billets are used for manufacturing of components. They used high-pressure interpass rolling to reduce residual stresses. However, there are associated limitations to achieve complex geometry and make it defect-free. They suggested that real-time temperature monitoring and feedback systems could minimise these issues [12].

Herzog et al. reviewed the influence of the thermal cycle on the different properties of the additively manufactured parts for laser beam, electron beam and plasma beam process. They also define the relation between process, microstructure and properties. The effect of thermal cycle and high cooling rates on grain structure are analysed [13].

Tapia et al. discussed the various temperature sensors that can be utilised for temperature measurement and real-time controlling of AM. The determination of material emissivity is very difficult, and this can be lead to inaccurate temperature measurement. Also, the AM setups are not equipped with the customised inbuilt monitoring sensor, which limits the process monitoring and real-time controlling [10].

Pan et al. discussed the recent research in additive manufacturing monitoring and controlling. They find the need for automation of the process. Also, there is further research in process control, and optimisation is required to control residual stress and distortion [4].

2.2 Tungsten Inert Gas Welding

Tungsten Inert Gas (TIG) or Gas Tungsten Arc Welding (GTAW) is a traditional method of welding for quality products. It is useful in many applications due to its capability to promote all three types of welding, namely autogenous, homogeneous and heterogeneous. Here this autogenous, homogeneous and heterogeneous welding process is referring to the process where no-filler material, the filler similar to the base material, and the filler different from the base material is used, respectively. Many researchers have widely studied this welding process for the welding of a broad range of material, including metals and alloys, to explore the various advantages and the process applicability [14–18]. This non-consumable electrode process is found useful in many other applications such as surface hardening, melting, alloying, cladding, additive manufacturing, etc. [19–27].

Kumar et al. performed surface modification in AISI 4340 steel by multi-pass TIG arcing process. They studied the effect of process parameters by varying arcing current and travel speed while keeping arc voltage constant at 10.5 ± 1.0 V. They found that the process improved the surface hardness and other mechanical properties. The magnitude of change in the property was dependent on the heat input [20].

Mustafa et al. modified the steel substrate surface with TIG welding. They reported that the alloying of SiC on the steel substrate could vary the hardness between 670 and 1165 Hv. They also observed that with high heat input, there is a difference between surface and inner part properties which induces residual stresses [26].

Orlowicz et al. performed the surface hardening of nodular cast iron by TIG remelting. The TIG current and scanning speed was varied in the range of 50–300 A and 200–800 mm/min, respectively. They observed that the surface hardness reduces with the increase of arc current. However, it increased with an increase in scanning speed for all current intensity studied. The increase in hardness due to fast solidification of superficial regions contributes to the crystallisation of cementite eutectic which transformed austenite present in the eutectic into partly martensite. They also observed that the remelting depth and width both increased with the increase of current intensity for all scanning speed [28].

Karamis et al. employed TIG melting and controlled chilling process to eliminate the graphite phase nodule from the cast iron. They found chilling process could not eliminate the graphite phases from nodular cast iron while an almost nodule-free surface was obtained by the TIG melting process. They reported that the depth and width of the change in microstructure could be controlled more effectively with an automated system [27].

The TIG has also been extensively used for surface cladding application due to its cost-effectiveness, ease of handling compared with other methods such as electroslag, laser, explosive, submerged arc cladding etc. [23,29].

Lv et al. compared the cladding of hot and cold copper wire on the steel substrate. An additional TIG arc was used for heating of the wire. They found that below 240 A the spreadability of hot wire was better than the cold wire. They also found that the cladding hardness improved with the increase of current and dependent on Fe content [23].

Guijun et al. used the laser for cladding purposes and concluded that the dilution of the powder is mainly dependent on the temperature of the weld pool. Also, the dimension of the clad layer is dependent on the temperature of the weld pool [29].

2.3 Temperature Monitoring

The emissivity is the ratio of emissive power of any physical body to that of the black body at the same temperature. The real body emissivity can vary with temperature, measuring wavelength spectrum, and the direction of emitted radiation. It also may differ at a specific wavelength over the temperature range. This effect is due to the spectral distribution of emitted radiation that varies with temperature. The single-channel pyrometer requires emissivity value for the true temperature measurement. However, in the case of ratio pyrometer, the requirement of the emissivity becomes almost negligible within the specific bandwidth of measurement. An error in temperature measurement could only appear if the surface emissivity varies in between working wavelength of the pyrometer [30–32].

Muller et al. developed a two-colour pyrometer for the temperature measurement of surfaces with varying emissivities. They presented the accuracy of one colour and the two-colour mode temperature measurement for aluminium alloy. They found that the wavelength range between 1.7 µm and 2.0 µm was giving the least error in measurement [30].

Forsythe et al. made a careful analytical study of the emissivity of tungsten from 0.30 µm to 4 µm range of an IR spectrum over a wide range of temperature from 927°C to 3127°C [31].

A.G. Worthing investigated emissivity of tungsten in the visible spectrum (for $\lambda = 0.476$ µm and $\lambda = 0.665$µm) over a temperature range from 927°C to 3027°C and found that emissivity variation is linear over the temperature range [32].

The emissivity measurement at lower temperature ranges between 27°C to 727°C using the transient calorimetric technique was done and reported by

Verret et al. They also compared the found results with theoretical results presented by **Parker et al.** for higher temperature range 727°C to 2727°C [33].

From the above literature, it could be concluded that finding the emissivity of any surface is a crucial and essential parameter. In this experimental study, an attempt has been made to determine the emissivity variation with temperature for tungsten. A ratio pyrometer was used with spectral ranges between 1.5-1.6 μm for channel 1 and 2.0-2.5 μm for channel 2. Since the ratio pyrometer almost eliminates the effect of emissivity variation with temperature, it gives reliable temperature. In this way, a reliable set of emissivity values was obtained for a temperature range of between 500°C to 1650 °C.

2.4 Objectives of the Present Research

- Minimise the measurement error in in-situ temperature monitoring, implementation and validation.
- Automate the non-programmable TIG welding power source for controlling the GTAW process.
- In-situ monitoring of the temperature of the weld pool or deposited bead-
    - To find the temperature variation during deposition.
    - To optimise the operating parameters such as voltage, current, wire feed.
- Controlling of the weld pool or deposited bead temperature-
    - For uniform deposition of material.
    - To obtain uniform properties.
    - To reduce excessive spatter.
    - Reduce the bulging of material at the start and end of welding.

2.5 Research Methodology

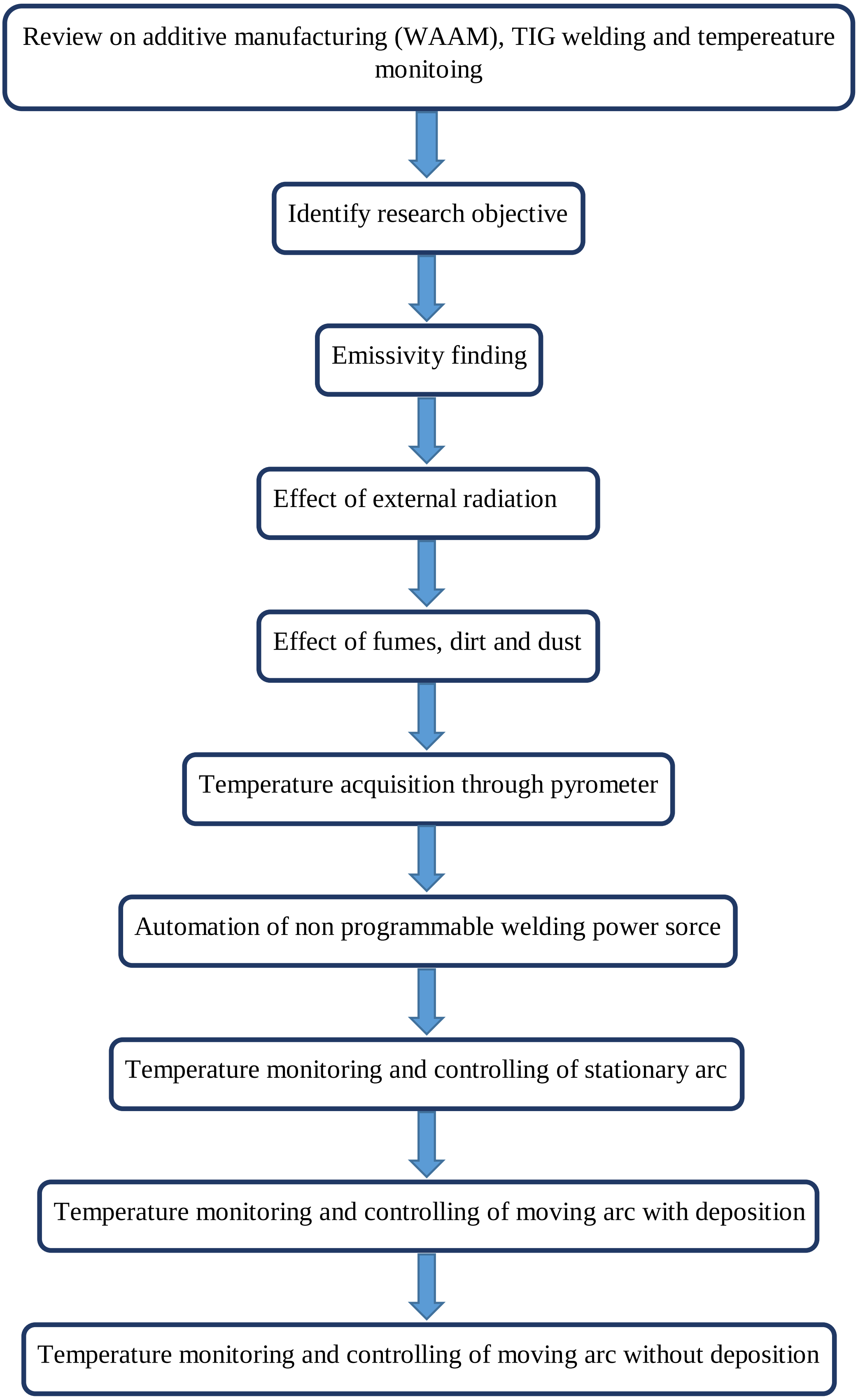

Chapter 3 Temperature Monitoring and Validation

3.1 Ratio Temperature Measurement

Manufacturing processes often involves heating of the material to a high temperature, which affects material properties significantly. So, it becomes essential to measure the true temperature of the material to monitor its properties accurately. Temperature measurement with single-channel pyrometer has many limitations, such as its high dependency on emissivity, media of measurement, the effect of external radiation, etc. The ratio pyrometer eliminates these limitations to a great extent as it is almost independent of the emissivity.

3.2 Emissivity Measurement

Figure 5 shows the experimental setup for the validation of the pyrometer. It consists of a halogen lamp, a DC power source, a pyrometer integrated with the processing unit, and a computer. The tungsten filament of the lamp (240 W, 24 V) was used as a target sample. The heating of the filament was controlled by a variable DC power supply. The filament was in a rectangular shape of width 4 mm and length 10 mm. Since the gap between intermediate coils was very less, it was assumed as a flat surface. The experimental setup for pyrometer temperature measurement is shown in Figure 6. The steel sample is heated with the help of a halogen lamp for a different set of experiment. However, a stainless casing of length 210 mm (focal length of the pyrometer) and opening of 8 mm was made in the house to prevent the pyrometer lens from the spatters and settling of fumes and dirt.

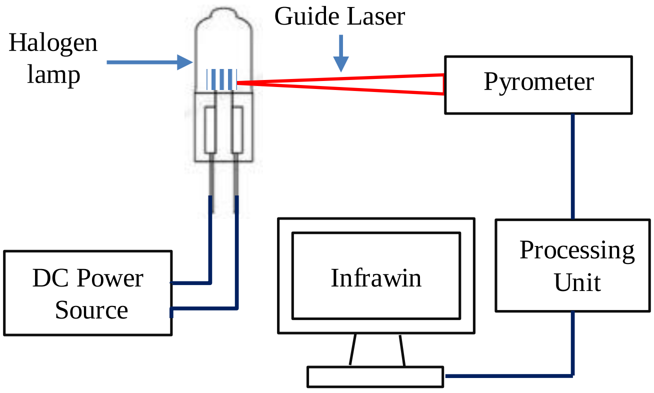

Figure 5: Pyrometer Validation Schematic

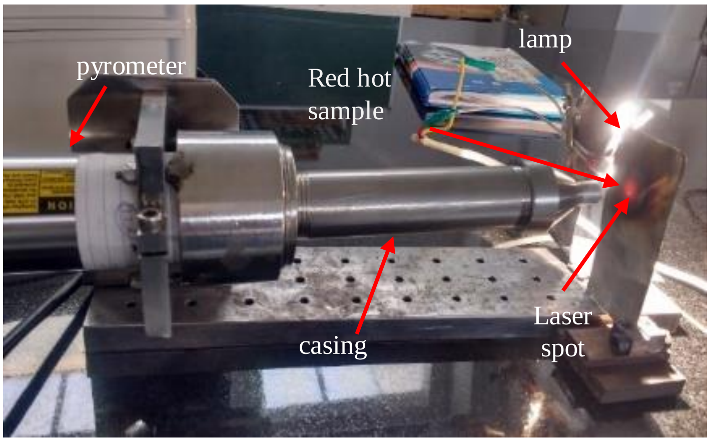

Figure 6: Pyrometer Validation Schematic And Experimental Setup

Infrared thermometer measures the temperature by sensing the infrared energy which every material or object will radiate at above absolute zero Kelvin (0 °K). It works on the principle Planck`s law of black body radiation by converting the spectral energy density R as a function of wavelength λ (m) and temperature T(K) [34]. The temperature is dependent on the emissivity factor of the heated surface. This dependency on emissivity could be minimised by employing the ratio pyrometer as it takes the radiation from two independent spectra. Therefore, the measured temperature using ratio pyrometer could be considered as more accurate [30]. The utilised pyrometer could be operated in both single-channel and two-channel ratio mode. Ideally, the measured body temperature should be identical for both the modes. However, in the case of single-channel mode, a known emissivity value need to be provided. Therefore, the temperature would change depending on the input emissivity value. It could be found that at a specific value of the emissivity for the single-channel mode, the measured temperature will become as same as the ratio mode. The value of this emissivity was obtained here, iteratively for a stabilised constant temperature Figure 7. The stair steps in Figure 7 represents the iteration performed in order to match the temperature. This procedure could be repeated to find the emissivity with respect to temperature for any unknown material.

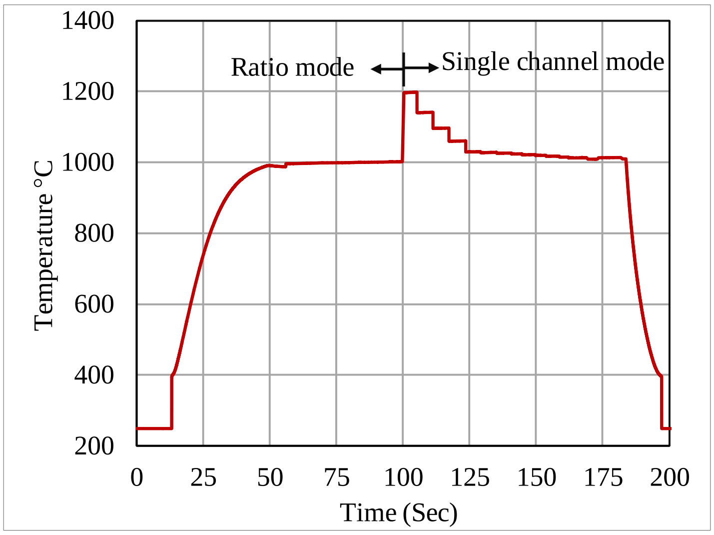

Figure 7: Emissivity Measurement Principle

Figure 8 and Figure 9 show the found emissivity curve for tungsten filament and graphite sheet. The emissivity points on a particular temperature are found iteratively using the above principle. The presented results are matching well with the reported emissivity using different approaches and controlled environment [35,36].

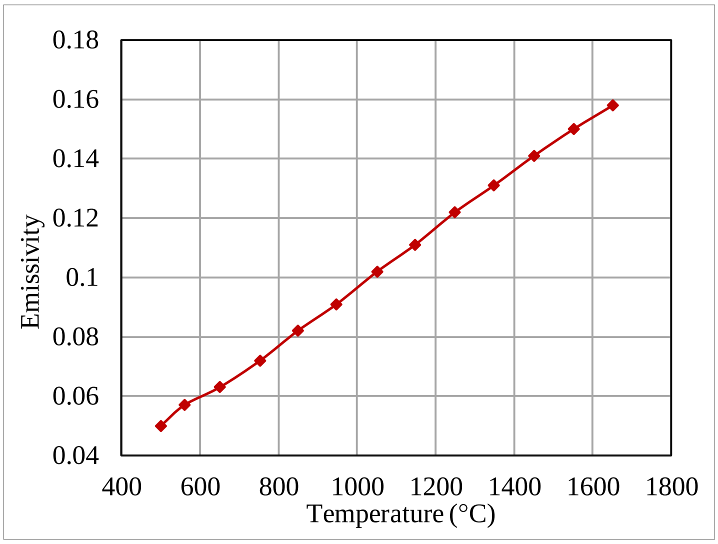

Figure 8: Variation In Emissivity Of Tungsten With The Temperature

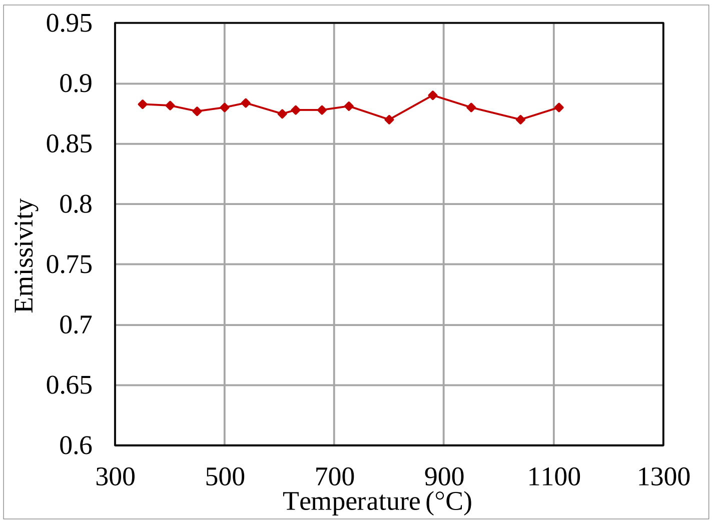

Figure 9: Variation In Emissivity Of Graphite With The Temperature

3.3 Effect of External Radiation

The manufacturing operations are often exposed to external radiation. These circumstances may affect the accuracy of the measured temperature. A series of experiments were performed to study the effects of these factors.

The external radiation may appear in the manufacturing environment from different sources. Therefore, it is essential to analyse and minimise the chances of errors. Both the modes of measurement was examined to find the deviation in temperature measurement due to external radiation. For the purpose, an additional lamp was introduced in the path of the measurement with an offset of about 100 mm, as shown in Figure 10. The filament temperature was measured in ratio mode first, and the temperature was allowed to stabilise. Then the other lamp was turned-ON. The similar experiment was performed for single-channel mode. From Figure 11, it was observed that the ratio mode showed little variation in temperature due to external radiation. The dynamic nature of the temperature signal was observed in the case of the single-channel mode.

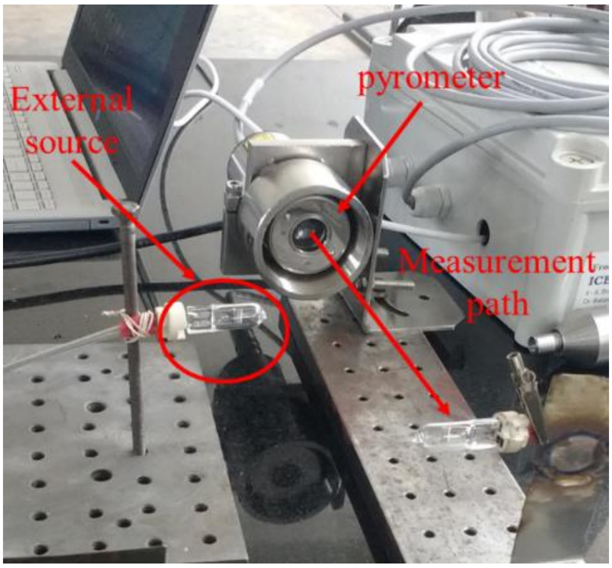

Figure 10: Effect Of External Radiation On The Temperature Measurement Experimental Setup

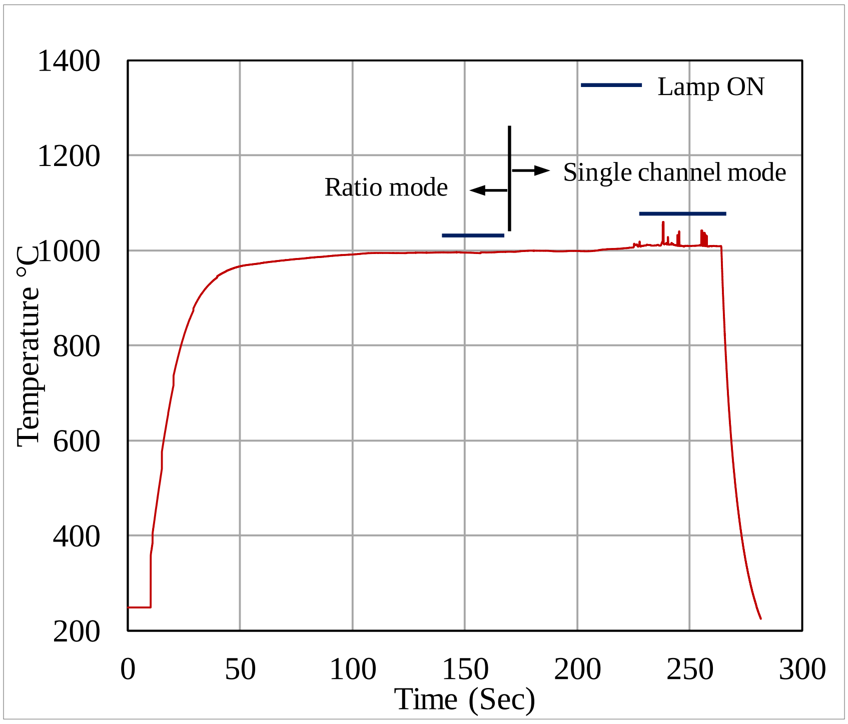

Figure 11: Time Vs Temperature Reading.

3.4 Effect of Fume, Dirt and Dust

The presence of the generated fumes, dirt or dust may also reduce the transmission of the radiation from measuring site to pyrometer and results in error in temperature measurement. Two ND (neutral density) filter were used to simulate a similar effect or block the known percentage of the radiation, as shown in Figure 12.

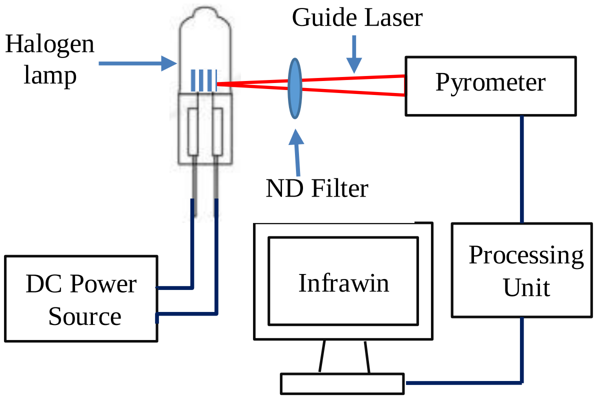

Figure 12: ND Filter Introduction Schematic

The chosen ODs (optical density) were 0.1 (80% transmission) and 0.6 (25% transmission), respectively. Here, the temperature was allowed to stabilise at different levels, and then the ND filter was introduced in the path of measurement. Figure 13 and Figure 14 shows the recorded temperature behaviour for both the mode of operation while using the ND filters. Figure 15 represents the percentage error for both the mode of operation at a different temperature. The error in the ratio mode of operation could be because of variation in transmission for the working wavelength of the pyrometer [37]. It was about 4% and 10% for ND filter of OD 0.1 and 0.6, respectively. This variation would affect the constant emissivity factor in ratio mode, which was reflected in terms of a marginal error. However, the recorded error was lesser in ratio mode compared to the single-channel mode of operation. It makes the ratio pyrometer a good choice for TIG based applications.

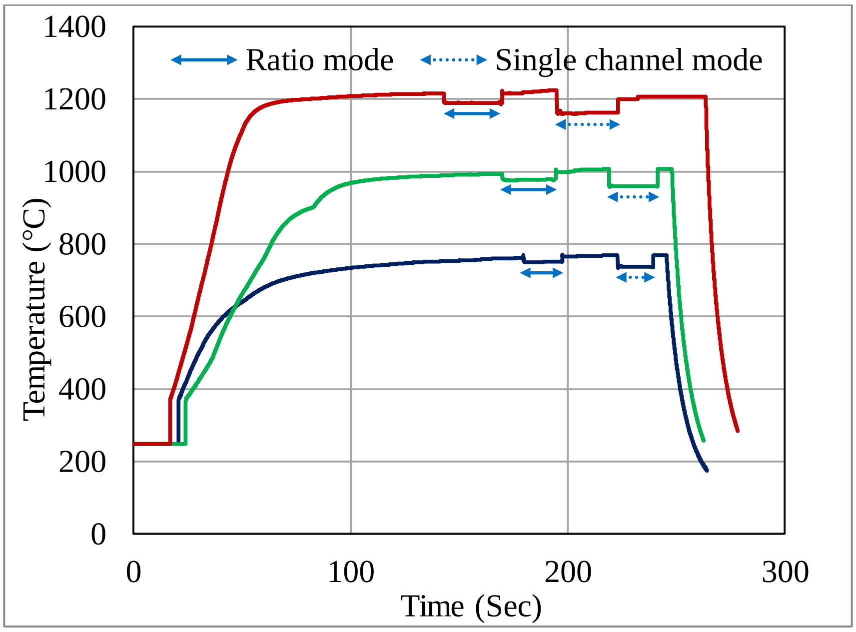

Figure 13: Effects Of ND Filters In Temperature Measurement At 0.1 OD (80% Transmission)

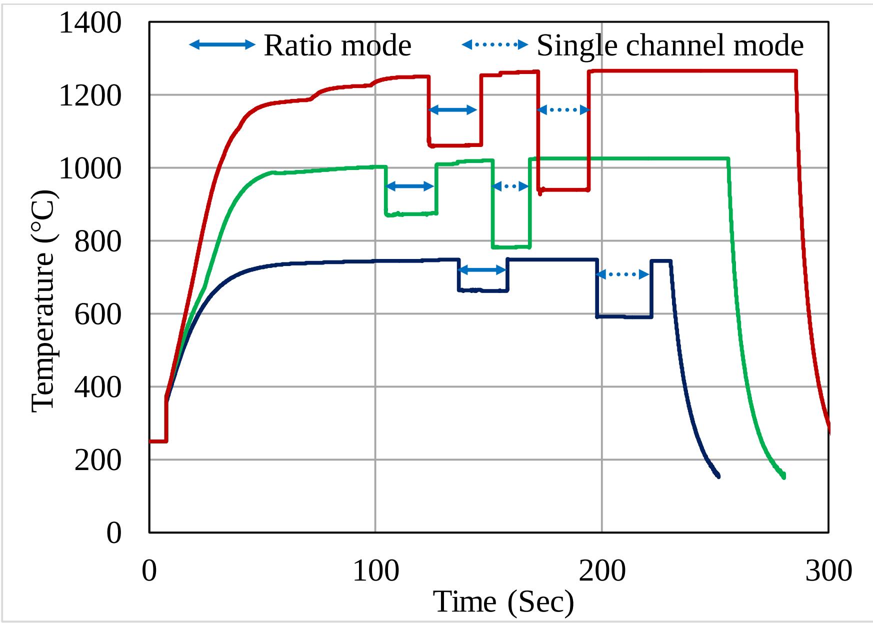

Figure 14: Effects Of ND Filters In Temperature Measurement At 0.1 OD (80% Transmission)

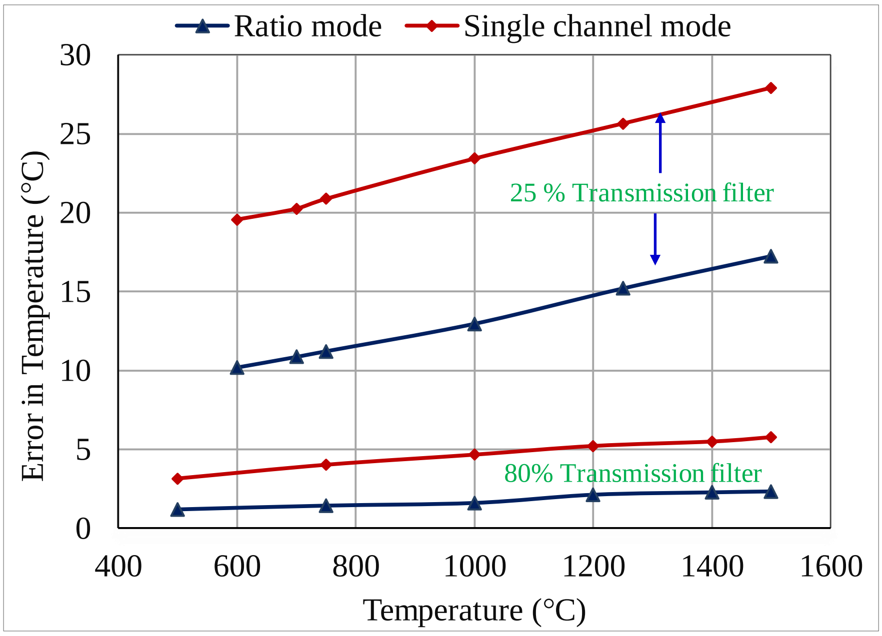

Figure 15: Percentage Error For Both ND Filters At Different Temperature.

3.5 Conclusion of temperature monitoring and validation

- Based on the conducted experimental study the following conclusion can be made
- The ratio pyrometer is a better choice for accurate temperature measurement.
- The measured temperature is unaffected by any external radiation.
- The emissivity of tungsten was found to have approximately linear proportional relation with temperature.

Chapter 4 Automation & Control

The automation and control of TIG welding are required to overcome the limitations in the manufacturing process, as discussed in chapter 2. Also, many of the above applications discussed in chapter 2 require controlled heating and melting of the material, which is difficult to achieve in case of manual operation. The harmful radiation of these welding process and related health issues also caused a significant reduction in skilled operators in the field. Further, the applications such as additive manufacturing, cladding, alloying, etc. require trivial control on the deposition parameter as it has to be taken from CAD (computer-aided design) model. However, the high cost of the programmable welding machine makes the process difficult to adopt for small to medium-sized industries. In this presented experimental work, a simple easy to adopt and cost-effective method has been developed which could enable the TIG welding machine to be programmable. A data acquisition system (DAQ) was used to bridge the communication between a computer and a welding machine or TIG power source. It was achieved by replacing the foot pedal control of the machine with a DAQ card. A feedback control system was implemented considering the generated temperature as a primary parameter. This feedback control regulates the input power to maintain the desired temperature at the desired location. A wide range of experiments was performed to establish the process such as temperature control at a different magnitude while keeping the TIG torch stationary, moving with the different speed and during single bead deposition.

4.1 Experimental Detail

The experiment was carried out with a 300A TIG (AC/DC) welding machine (make: Kemppi, model: MasterTig MLS 3003ACDC) as shown in Figure 16. It was equipped with the standard features such as HF (high-frequency) start, the remote control using a foot pedal, and manual control to set the arc current. A straight neck air-cooled torch was used for the purpose. This type of torch is desirable for automated systems for ease of mounting on CNC (Computer Numerical Control) machines for automated welding. The utilised electrode was 2% thoriated tungsten electrode of diameter 2.4 mm. Argon gas was used as an inert gas at a constant flow rate of 10 l/min. All the experiments were conducted on the DC mode of operation, keeping the straight polarity (DCEN- Direct Current Electrode Negative). Stainless steel (SS316) sheet of thickness 1.5 mm and mild steel sheets of 3 mm were used as the substrate for different experiments.

Figure 16: GTAW Setup

A DAQ system (NI USB-6001), as shown in Figure 17, was used to bridge the communication between a computer and the TIG source. It was achieved by replacing the foot pedal control of the machine with the DAQ and control the reference 0–5V. The LabVIEW software was used for the appropriate programming.

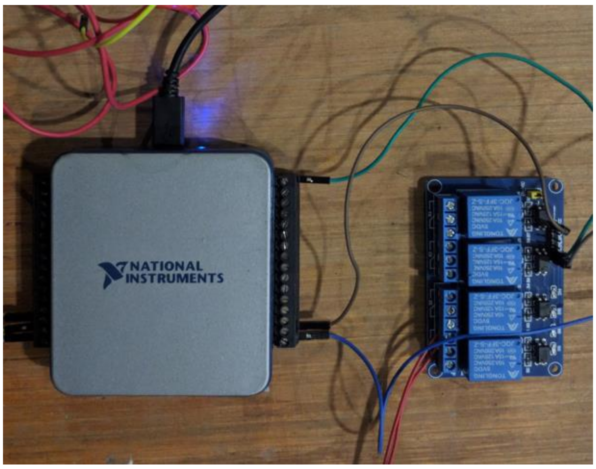

Figure 17: Data Acquisition System With Relay

The first attempt for automation was made with the help of digital potentiometer X9C103, as shown in Figure 18. It is a 10k ohm digital potentiometer which divides 10k ohm total resistance into 100 steps. Each step is of 100 ohms. The digital potentiometer replaced the mechanical potentiometer of the foot pedal.

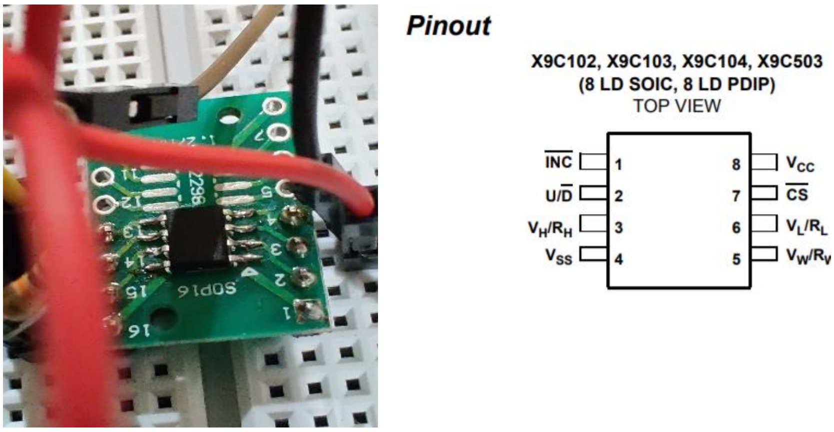

Figure 18: Digital Potentiometer and its Connection

The temperature control was introduced after the successful implementation of the programmable control of the TIG power source. A non-contact two colour (ratio) pyrometer (make: LumaSense Technologies, model: IGAR-6 Advanced) was used to monitor the in-situ temperature. The working wavelengths of the pyrometer were 1500–1600 nm and 2100–2500 nm for channel-1 and channel-2, respectively. It can also be operated in a single-channel mode where radiation from the entire spectrum of both the channels is considered. The minimum response time of the pyrometer is 2 ms, and the working temperature ranges from 250°C to 2000°C in ratio mode and 100°C to 2000°C in single-channel mode, respectively. The pyrometer has visible laser sighting for focusing the target object for temperature measurement with a minimum spot diameter of 2.1 mm at a distance of ~210 mm. The advantage of using this type of pyrometer is that it could also be communicated through provided ASCII codes [38]. A feedback control system was implemented, taking the temperature as an input parameter.

4.2 Automation of Non-programmable Welding Power Source

The automation of the welding power source can be done by understanding the basic construction of manually operated foot pedal. The basic construction helps in to understand the working principle of the foot pedal. The basic construction shows a switch and potentiometer was used to control the machine manually. To switch from manual to computer control the DAQ system and a Relay was used to control the power source using the LabVIEW platform. The implementation of this system was checked by an experiment whereby changing input reference voltage changes the output power.

4.2.1 Foot Pedal Construction

The basic construction of the TIG machine allows the user to ignite and control the arc current using the foot pedal. This foot pedal is used to control the TIG system remotely. Figure 19 shows the foot pedal schematic construction and circuit diagram.

(a)Foot pedal

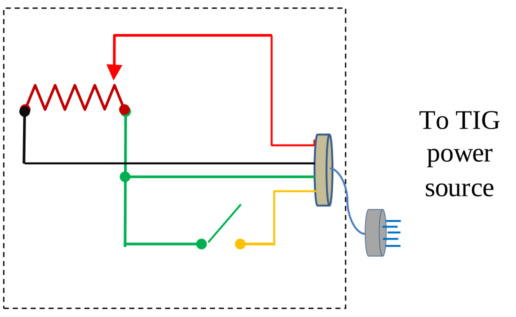

(b)circuit diagram

Figure 19: Foot Pedal (A) Schematic (B) Circuit Diagram

It consists of a mechanical switch and a potentiometer. It is positioned inside the pedal in such a way that with an application of load the switch would be operated first and then the potentiometer. This switch ON or OFF position enables or disable the foot pedal, respectively. The ON position also enables the inert gas flow, which is required for arc stabilisation. Further continuation of the load mechanically regulates the potentiometer and defines the input welding current.

4.2.2 Working Principle of Foot Pedal

Primarily the foot pedal regulates the reference DC voltage varying in the range of 0–5 V instead of the actual TIG parameter available at the torch for welding. Here, the '0V' represents the minimum and '5V' the maximum set TIG current, respectively. With the application of the load on the pedal, the potentiometer wiper position changes which defines the resistance and hence reference voltage. In general, this resistance varies in the range of 0–10 kOhms. Figure 20 shows a schematic of the pedal at "No-Load" condition. This condition keeps the switch to OFF; hence no TIG operation would take place.

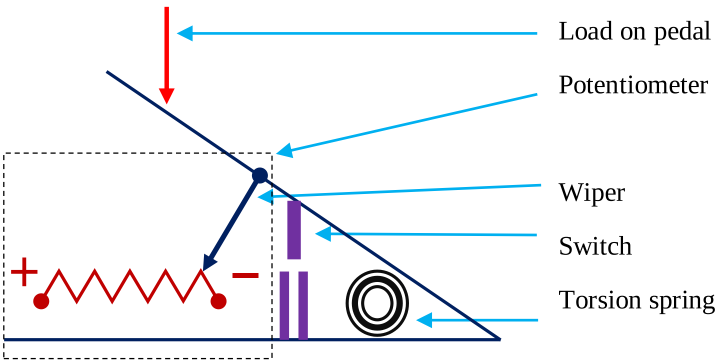

Figure 20: Schematic Of The Construction Of Foot Pedal With No-Load

Figure 21 (a) shows the condition when the pedal is just pressed; it enables the switch to ON and triggers the inert gas flow. However, at this condition, the wiper position remained at minimum resistance. This minimum resistance sends the signal to the TIG machine in terms of the reference voltage (usually lower end of 0–5V), which regulates the TIG current to its minimum possible magnitude available with the machine.

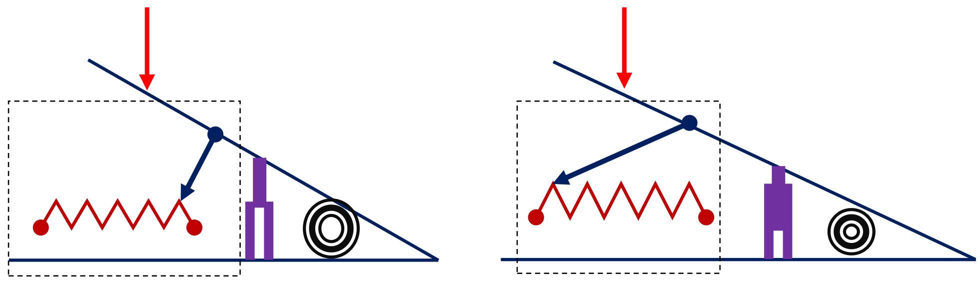

(a) *(b)*

Figure 21: Schematic Of The Construction Of Foot Pedal With An Illustration Of (A) With-Load, Condition And (B) Regulation Of Potentiometer Resistance.

Figure 21 (b) shows the condition when the pedal is further pressed. Here, depending on the load and the position of the potentiometer wiper, the reference voltage would be regulated, and TIG current would be available at the torch. These different conditions of operation are also presented in Table 2 for better understanding.

Table 2: Working principle of the foot pedal.

Pedal position	**Switch (ON/ OFF)**	**Potentiometer resistance**	**Reference voltage**	**TIG current (available at torch)**
Not pressed	OFF	Not active	None	None
Just pressed	ON	Active	Minimum	Minimum (arc ignition)
Positioned in-between	ON	Relatively higher	Medium	Medium
Completely pressed	ON	Maximum	Maximum	Maximum

Note: Since this foot pedal is operated manually, the exact value of resistance or reference voltage remains unknown. Therefore, the terms such as not active, active, relatively higher and maximum were used to represent the different condition of it.

4.2.3 Enabling Computer control In TIG Using Digital Potentiometer

The foot pedal consists of a mechanical potentiometer and a switch. In the first attempt, the mechanical potentiometer was replaced by a digital potentiometer, and the mechanical switch was replaced by the relay, as shown in Figure 22.

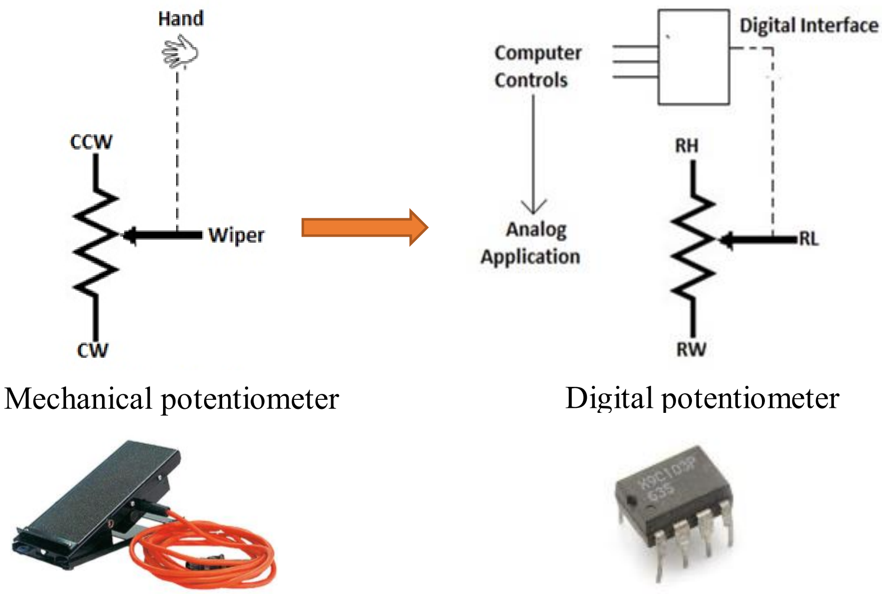

Figure 22:Mechanical potentiometer replacement with the digital potentiometer

The digital potentiometer consists of 8 pins, as shown in Figure 23. The figure shows the connection pins of the digital potentiometer. INC pin takes a square wave whose ON state is 5v, and OFF state is 0v.

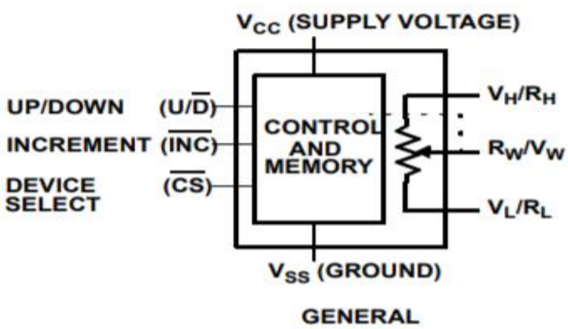

Figure 23 Block Diagram Of Digital Potentiometer

U/D pin controls the direction of movement of the wiper. Vcc and Vss are 5v and ground pins, respectively. CS pin turns on and off the potentiometer. V_H

and V_L are the voltages that need to be divided. V_W is the wiper terminal of potentiometer. Whenever there is a high to low transition on the square wave, it results in the movement of wiper whose direction is decided by the U/D pin.

The digital potentiometer is imitating the working of a mechanical potentiometer of the foot pedal. Using a breadboard; INC, U/D, Vss pins of digital potentiometer was connected to DAQ card. The square wave is sent by DAQ card to INC pin as per requirement. A different pin of DAQ card controls U/D pin. The 5v and 0v wires coming out of TIG welding machine was connected to V_H and V_L pins of Digi-pot. Wiper wire of machine was connected to V_W pin. An extra mechanical relay has been used to switch on and off the gas connection. A pyrometer has been used for temperature measurement as the sample being heated by the welding torch of the TIG welding machine, as shown in Figure 24.

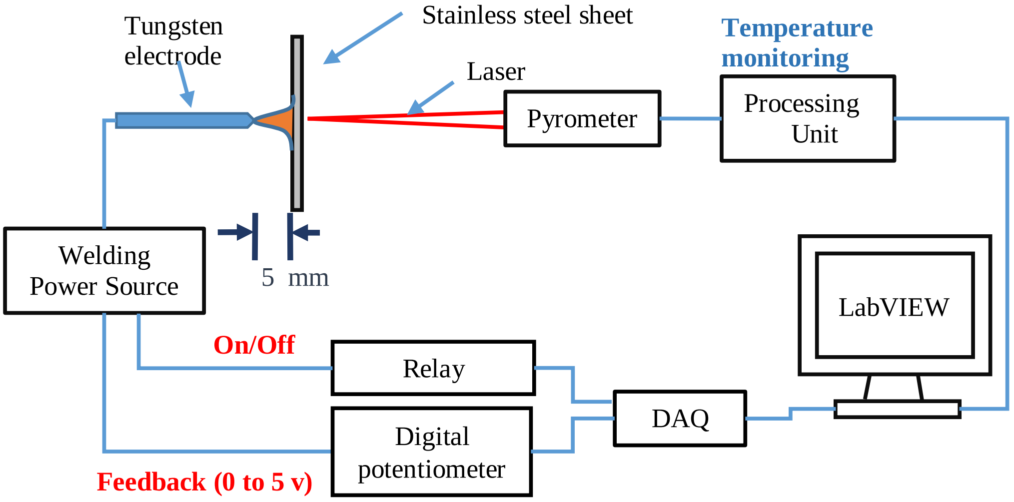

Figure 24 Schematic of feedback control using a digital potentiometer

The temperature acquisition and feedback control are made with the help of the LabVIEW front panel, as shown in Figure 25. It has instrument control which is used to communicate with the pyrometer. Once communication established, it acquires temperature and based on the temperature controlling signal generated to control the digital potentiometer resistance, which further controls the power output from the welding machine.

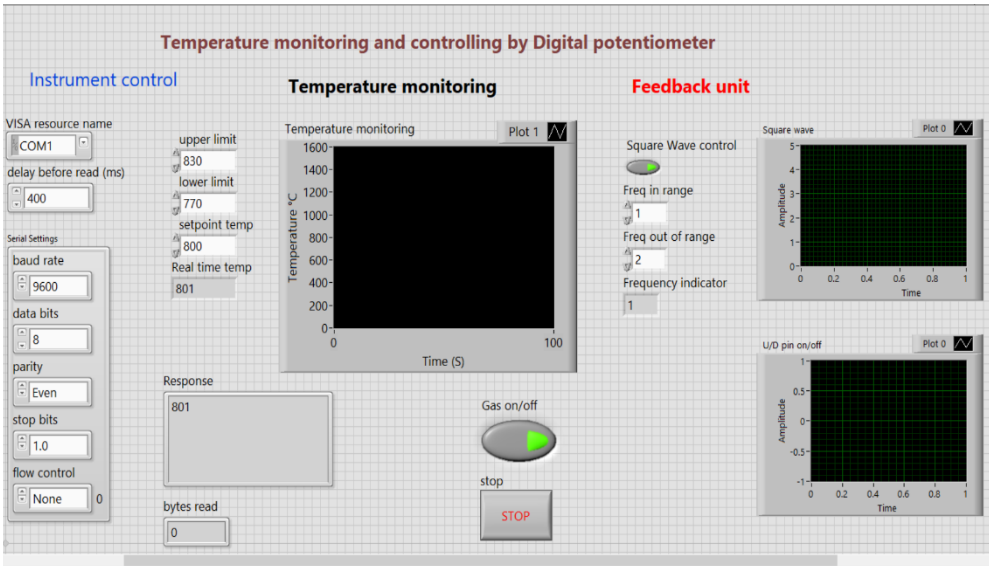

Figure 25 Front panel of feedback control using a digital potentiometer

The temperature measurement and control through the front of the heated sample is presented in Figure 26. The different temperature 800°C, 900°C, 1000°C and 1100°C was controlled with the help of a developed control system using a digital potentiometer.

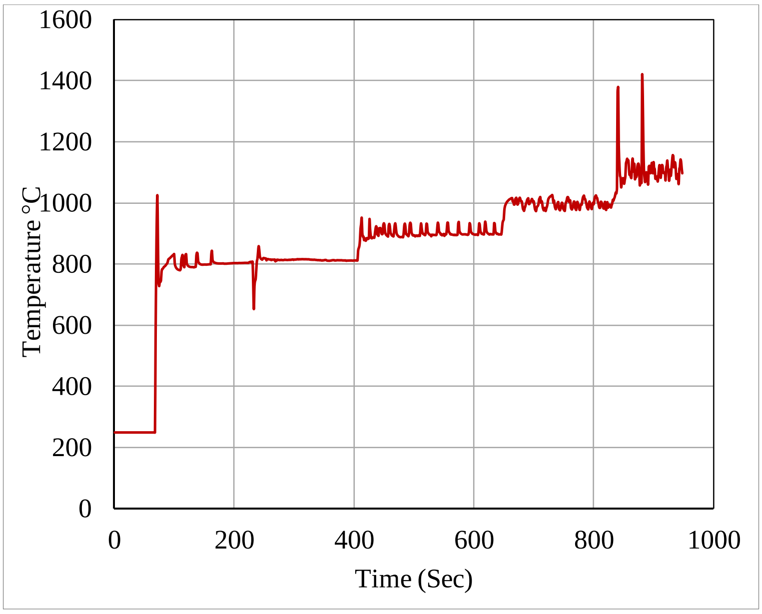

Figure 26 Temperature Vs Time Graph

The control of the arc energy was achieved successfully by using a digital potentiometer. However, a few limitations of the system was observed, which are as follows.

1. It takes a long time (2–3 sec) to respond against the controlling signal.

2. In case welding process the temperature changes rapidly, so when the temperature goes beyond controlling limit, the potentiometer acts as a switch and either ON or OFF the arc. This switching further makes difficulties in controlling the temperature.

Therefore, the digital potentiometer was replaced with an analog output of DAQ and 0 to 5-volt signal using was directly given to the wiper of the welding power source using a PID controller.

4.2.4 Enabling Computer Control in TIG using PID

The mechanical work involved in a foot pedal needs automation for precise variation of the reference voltage, or, replacing the pedal with external control could make the system automated. Figure 27 shows the schematic of the circuit, which replaces the foot pedal with a DAQ system to communicate with the machine and also to control it. The analog output (AO) of the DAQ was used as a reference voltage required to control the arc current. The mechanical switch of pedal replaced by a relay and controlled by the digital output (DO) of DAQ. A relay which could be triggered using digital output (DO) of the DAQ was the replacement for the mechanical switch.

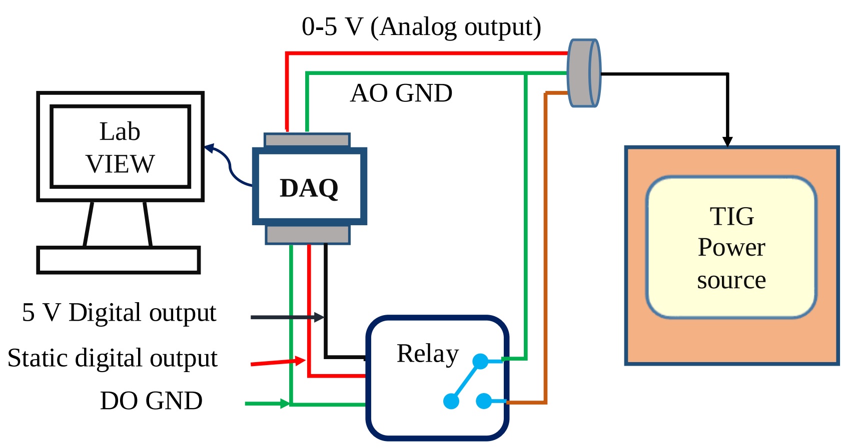

Figure 27: Schematic Diagram Of The TIG Automation.

4.2.5 Reference Voltage and TIG Current Relation

It is to be noted that the foot pedal only regulates the manually set maximum TIG current in the power source. A study was conducted to analyse the variation in the set TIG current when regulated through the DAQ system. A dedicated program was written to perform this study shown in Figure 28.

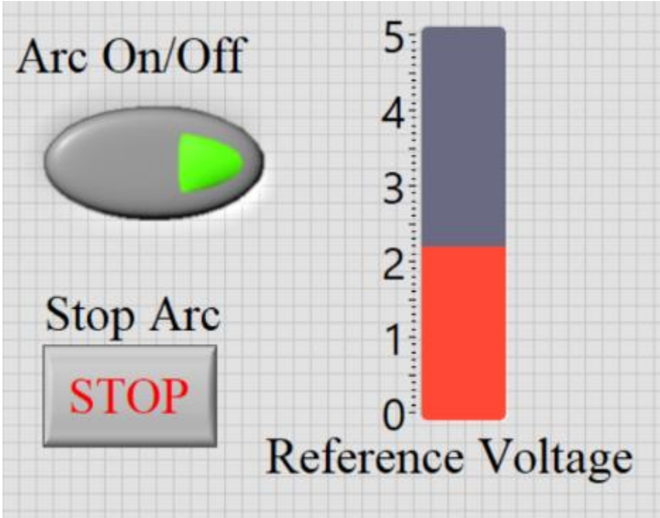

Figure 28 Labview Front Panel For Controlling The TIG

Figure 29 shows the variation in TIG current for four different conditions of reference voltage for the maximum set current of 52 Amp. The reference voltage was varied, and the obtained TIG current was noted from the display.

(i) (ii) (iii) (iv)

Figure 29: (I) RF Set To 0V, (Ii) RF Set To 0V, Relay ON- Inert Gas ON, (Iii) RF Set To 2.5V, (Iv) RF Set To 5V. *RF- Reference Voltage.

The experiment was extended for five different set current of 30, 50, 70, 100 and 150 amps, and plotted in Figure 30. Here the reference voltage was varied with an increment of 0.1V to analyse the precise variation the obtained TIG current. It was observed that the output TIG current increases with an increase of reference voltage and has almost linear relation.

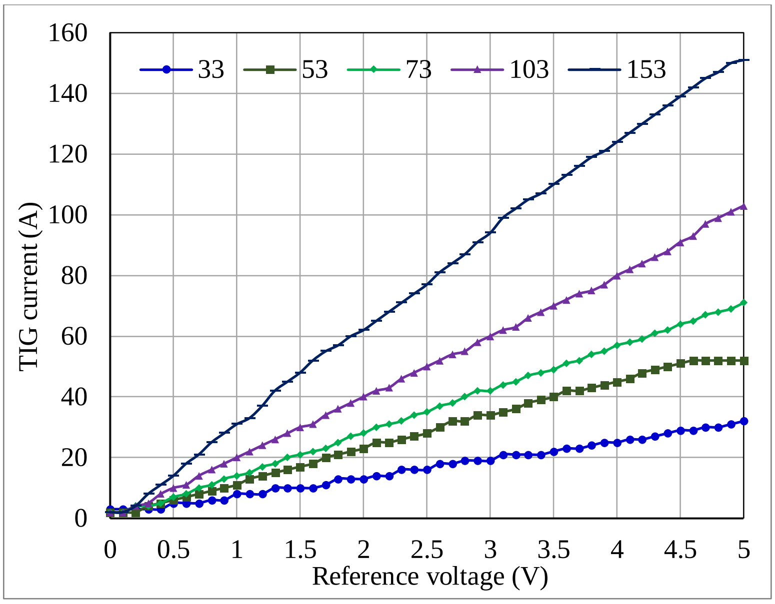

Figure 30: Variations In TIG Current With Reference To The Input Reference Voltage

4.2.6 Implementation of The Temperature-Dependent Feedback Control

A dedicated LabVIEW program was written to communicate with the pyrometer outside the provided software (Infrawin) from the manufacturer. It contains mainly three parts, i.e. instrument control, in-situ temperature monitoring and feedback control from the same program. It was achieved by bridging the communication with the help of virtual instrument software architecture (VISA) and communicating through it via ASCII codes. Figure 31 shows the front panel of the LabVIEW interface, where the real-time temperature measurement can be recorded. It also gives the temperature reading as numerical data which can be used as input data for the calculation of feedback control. An inbuilt PID (Proportional–Integral–Derivative) function of the LabVIEW was used to send the feedback signal based on the setpoint temperature. The generated feedback signal was communicated to the TIG welding power source using the DAQ to control the arc current and hence the temperature.

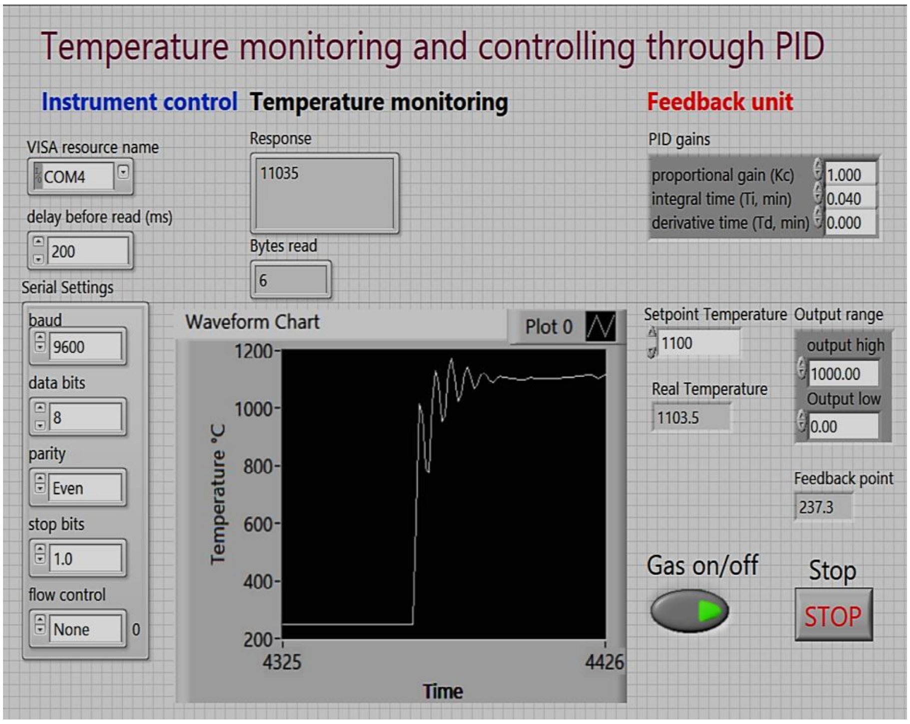

Figure 31 LabVIEW Front Panel For Temperature Measurement And Feedback Control.

4.3 Temperature-Dependent Feedback Control for Stationary Heat Source

Figure 32 shows the schematic of the experimental setup, where the TIG torch was kept stationary and targeted to a test sample. The generation of arc done manually instead of high frequency (HF) starts because it can disturb the electronic equipment used in the experiment. The stand of distance (SOD) between torch and sample is maintained about 5 mm. The pyrometer was focused on the sample just behind the arc with the help of a guide laser. The temperature is acquired in LabVIEW with the help of the ASCII code. The developed program in LabVIEW generates a feedback signal with the help of virtual PID (proportional integral derivative). The DAQ is used to on/off the arc and at the same time generates 0 to 5 V reference voltage to regulate the power of arc.

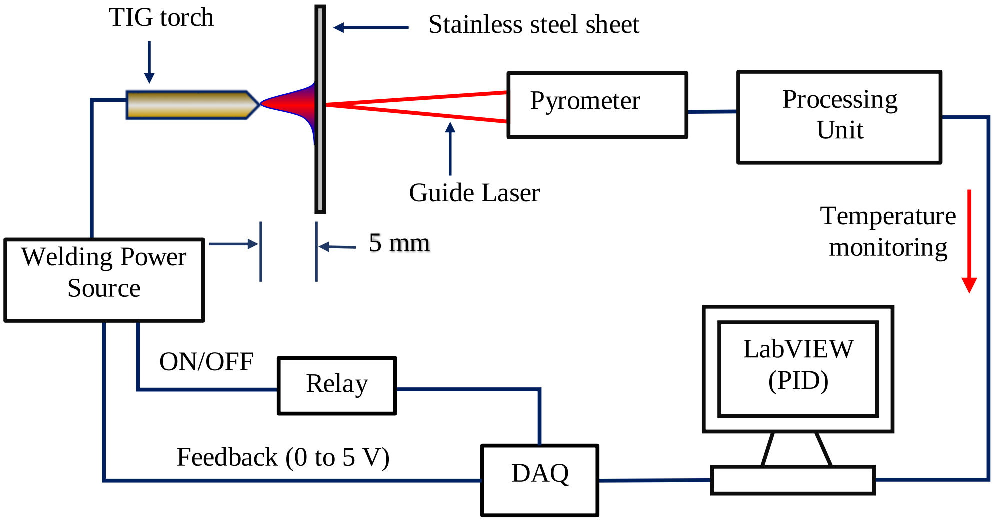

Figure 32: Schematic Of The Experimental Setup For The Controlling Of Stationary Heat Source

the experimental setup for the controlling of a stationary arc is shown in Figure 33. Two sets of experiments were performed with this experimental setup. In the first set, the pyrometer was focused on the sample, which was in-line with the tip of the electrode. In the second set of the experiment, the pyrometer was focused offset from the tip of the electrode of about 8 mm.

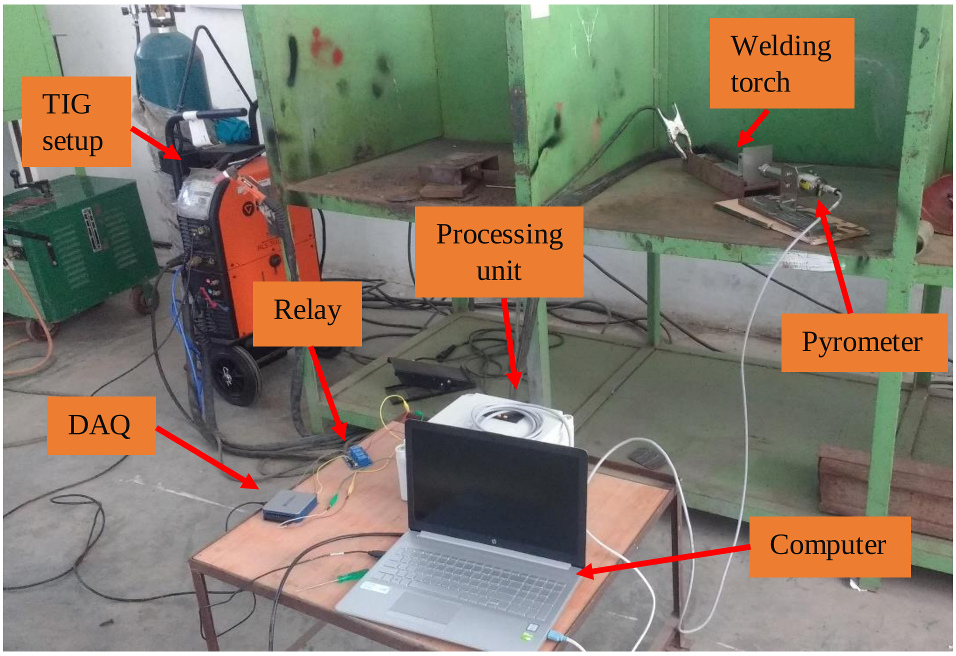

Figure 33: Experimental Setup For The Controlling Of Stationary Heat Source

4.3.1 Pyrometer was Focused In-Line with the Tip of the Electrode

the pyrometer was focused on the sample, which was in-line with the tip of the electrode, as shown in Figure 34. the pyrometer was focused on the middle of the red hot zone.

Figure 34: Pictorial View When The Pyrometer Was Focused In-Line

Figure 35 shows the recorded controlled temperature with respect to the time. The setpoint temperature was varied from ~600°C to ~1300°C with an increment (Figure 35a) and decrement (Figure 35b) of 100°C. The setpoint temperature was changed after each ~100 sec. It was chosen to allow the TIG source to stabilise the temperature. The utilised PID constants were found thorough iteration to achieve the optimum result. It was 1.0, 0.04 and 0.00 for proportional, integral and derivative, respectively.

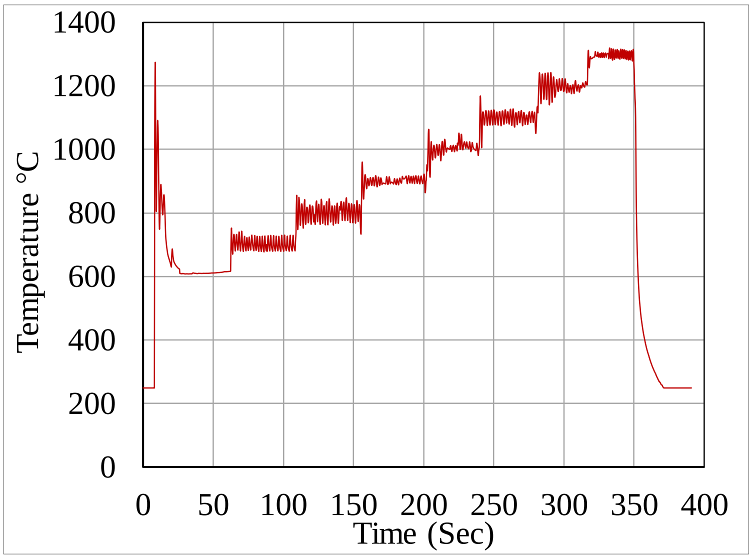

(a)

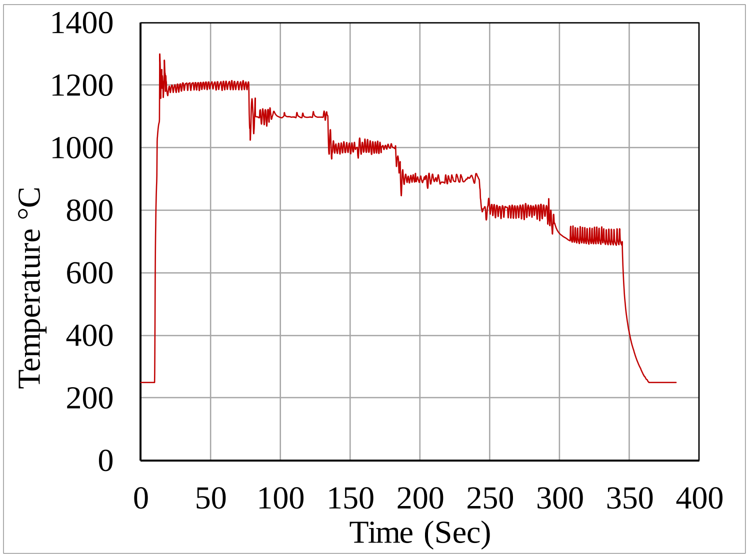

(b)

Figure 35: The Incremental And Decremental Controlled Temperature With Respect To The Time When The Pyrometer Was Focused (A) And (B) In-Line

4.3.2 Pyrometer Was Focused at an Offset With The Tip of The Electrode

the same experimental setup used in section 4.3.1 is used for temperature measurement and controlling of stationary arc except the pyrometer is focused at an offset of 8 mm as shown in Fig. 36.

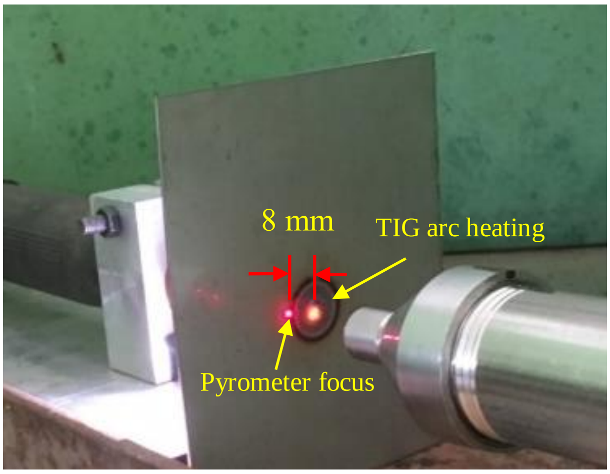

Fig. 36 Pictorial View When The Pyrometer Was Focused At An Offset Of ~8 MM With The Electrode

The recorded controlled temperature with respect to the time is shown in Figure 37. The setpoint temperature was varied from ~600°C to ~1300°C with an increment (Figure 37a) and decrement (Figure 37b) of 100°C. The setpoint temperature was changed after each ~100 sec. The PID constants are the same as the above experiment.

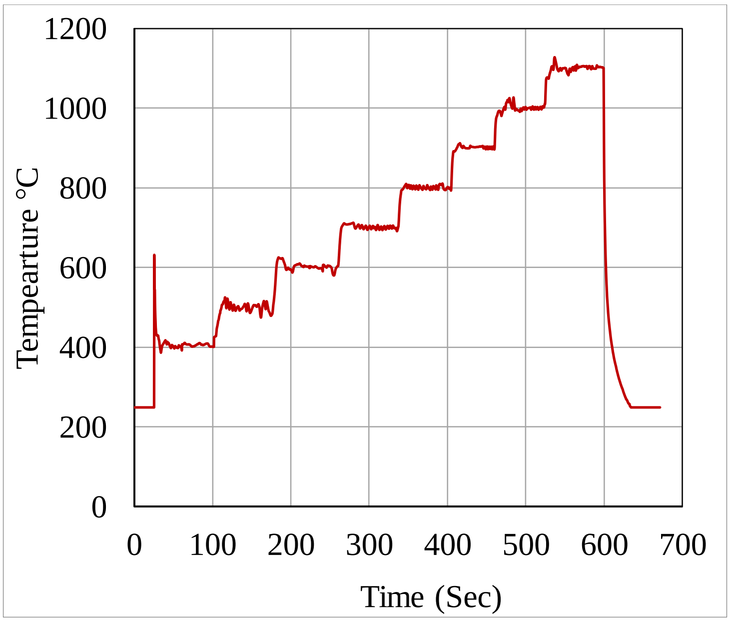

(a)

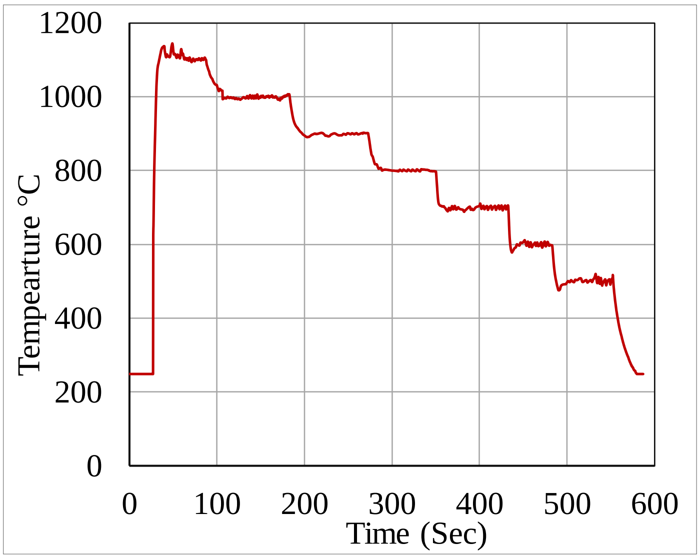

(b)

Figure 37: The Incremental And Decremental Controlled Temperature With Respect To The Time When The Pyrometer Was Focused (A) And (B) At An Offset

4.3.2 Conclusion of Temperature-Dependent Feedback Control for Stationary Heat Source

It was observed that the temperature was in the range of the desired setpoint for both the sets of experiments. In case of the first set of the experiment (when the pyrometer was focused in- line with the electrode), the stabilisation in temperature for above 1200°C and below 700°C could not be achieved for decremental control. It is because of the proportional constant of the PID, which overshoots the temperature above melting and causing the piercing of the sample for the setpoint of 1300°C. However, in the case of below 700°C, the sample could not be able to dissipate the heat more quickly as the bulk temperature increased due to decremental change in the setpoint temperature. A similar effect was observed, in the case of the second set of the experiment (when the pyrometer was focused offset with the electrode or conducted temperature control), the stabilisation in temperature above 1100°C could not be achieved for both incremental and decremental control. However, in this case, decreasing setpoint temperature of up to 500°C was achieved successfully. The calculated standard deviation in controlled temperature was found to be in the range of ±16°C and ±06°C, respectively, for in-line and offset focused control. This deviation was found to remain almost constant for both increasing and decreasing temperature control. The marginal higher deviation in the case of in-line focused control could be because of the instability of voltage in the sustained arc column. This instability in voltage could be considered as an inherent property of the process which remains exist despite keeping all the parameters (stand-off-distance (SOD), gas flowrate, current) constant [39].

4.4 Temperature-Dependent Feedback Control for Moving Heat Source

The moving arc control was difficult than stationary arc controlling due to the movement of the heating point. Also, the temperature measurement side is same as of arc. Figure 38 shows the schematic of the experimental setup for temperature-dependent feedback control for the moving heat source.

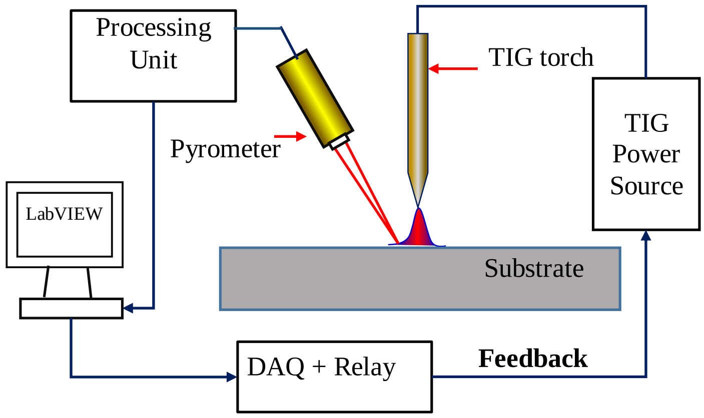

Figure 38: Schematic Arrangement For Moving Heat Source Temperature Control.

A 3-axis gantry CNC stage developed inhouse was used for the purpose. TIG torch and pyrometer was mounted on the Z-axis, and the target heating sample was mounted on the XY motion plate, as shown in Figure 39. This arrangement keeps the torch and pyrometer stationary for a constant SOD which minimises the chances for errors due to vibration. The pyrometer was focused at 12 mm behind the arc to promote the offset focusing to minimise the error in controlled temperature as found in the previous set of experiment. However, it was ensured that it always follows the heating seam. The feedback control was implemented for single track heating for different temperature. The scan speed and SOD were kept constant throughout the experiment at 60 mm/min and 4 mm, respectively. The PID constants were kept the same as the previous set of experiment.

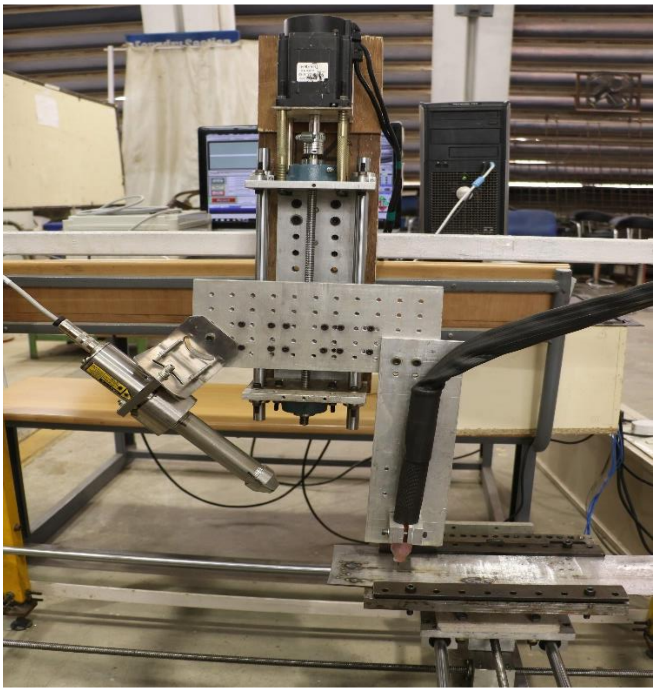

Figure 39: Experimental Setup For Moving Heat Source Temperature Control

The setpoint temperature was varied in three different ways between 1000°C to 1600°C to claim that the controlling is done in any condition. The recorded controlled temperature with respect to the time is plotted for a different set of experiments. First, incremental only (1000-1100-1200-1300-1400 °C, Figure 40a), second decremental increment and decremental (1200-1100-1000-1400-1300-1200 °C, Figure 40b), and third incremental decremental (1400-1500-1600-1500-1400 °C, Figure 40c).

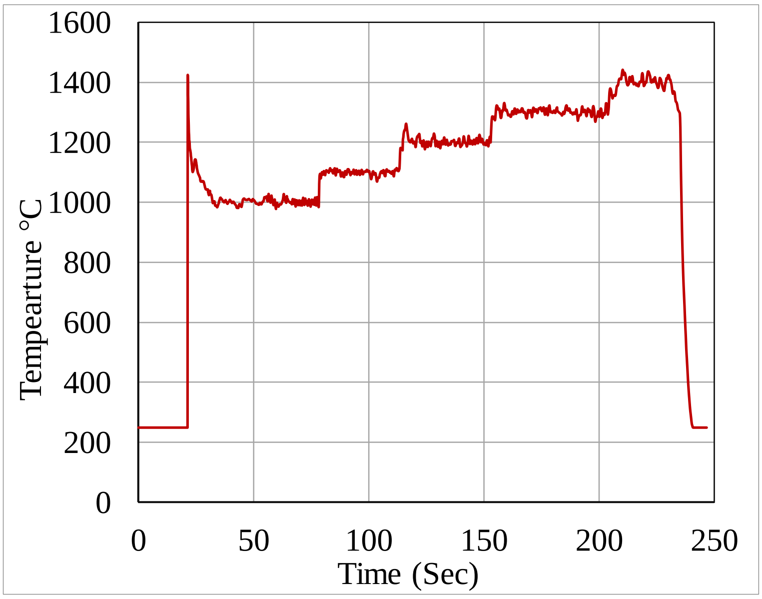

(a)

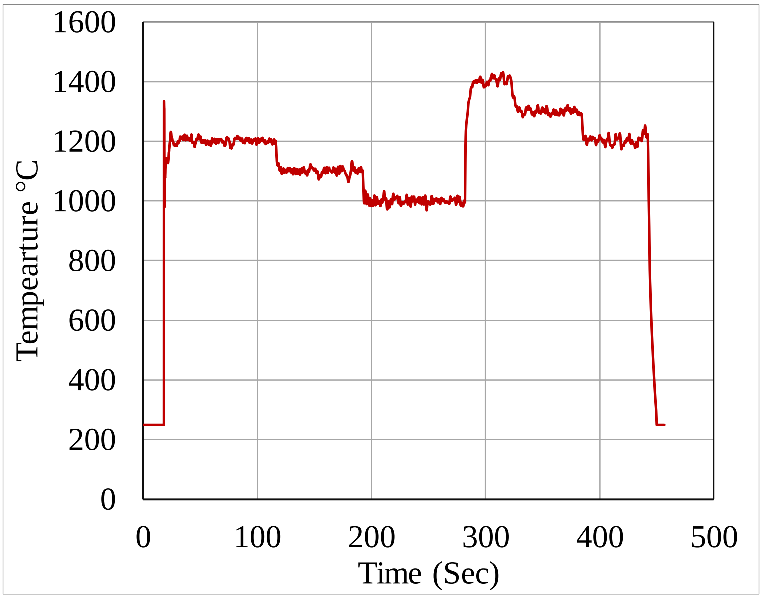

(b)

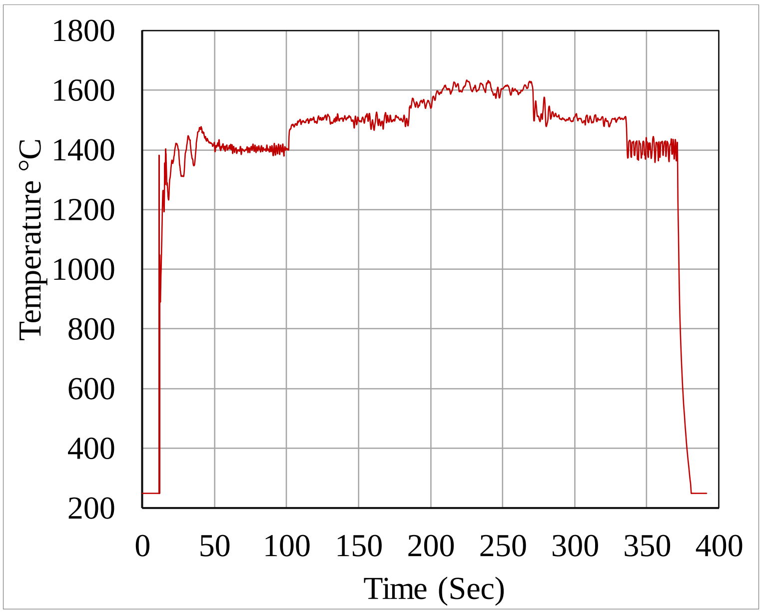

(c)

Figure 40: Feedback Temperature Control For The Moving Heat Source For (A) Incremental (B) Decremental-Increment- Decremental, And (C) High Range Temperature Control For Both Incremental And Decremental.

It was observed that the generated seam temperature due to TIG arc was within the setpoint for all sets of the experiment. In all three cases, the calculated standard deviation in controlled temperature was found to be in the range of ±15°C. This broad range of temperature control for surface heating may find many applications in industries such as surface modification, hardening, melting, etc. Also, it could be implemented only in the required area/ point of interest.

4.5 Temperature-dependent feedback control for the single bead deposition

The schematic and experimental arrangement for the temperature-dependent feedback control during single bead deposition is presented in Figure 41, and Figure 42, respectively. A 0.8 mm diameter steel wire (ER70S-6) was fed into the stabilised arc of TIG with the help of a cold wire feeder (make: ATE welding and model: SB-10-L). Front feeding (opposite to the direction of deposition) was adopted and maintained constant throughout the experiment at a constant feed speed of 1.5 m/min. Whereas the pyrometer was focused on the deposited bead at 12 mm behind the arc. It was kept at a near-vertical position behind the arc, to maximise the gain (radiation) which would be relatively scattered in the curved bead profile and striations.

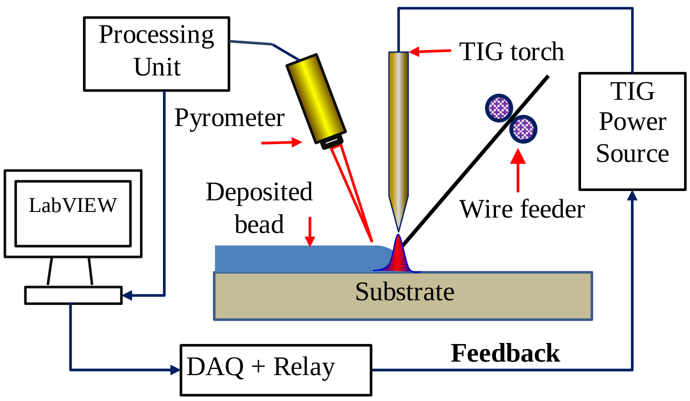

Figure 41: Schematic Arrangement For Deposition Of Single Bead Temperature Control

The experiment was performed at four different deposition speed, namely 150, 200, 250 and 300 mm/min. These deposition speeds were optimised based on trial experiments to obtain the continuous and uniform bead. It was observed that the reduction of deposition speed below 150 mm/min, causing overheating of the wire and the base plate, causing non-uniform bead formation, whereas, exceeding the speed above 300 mm/min leads to discontinuous deposition.

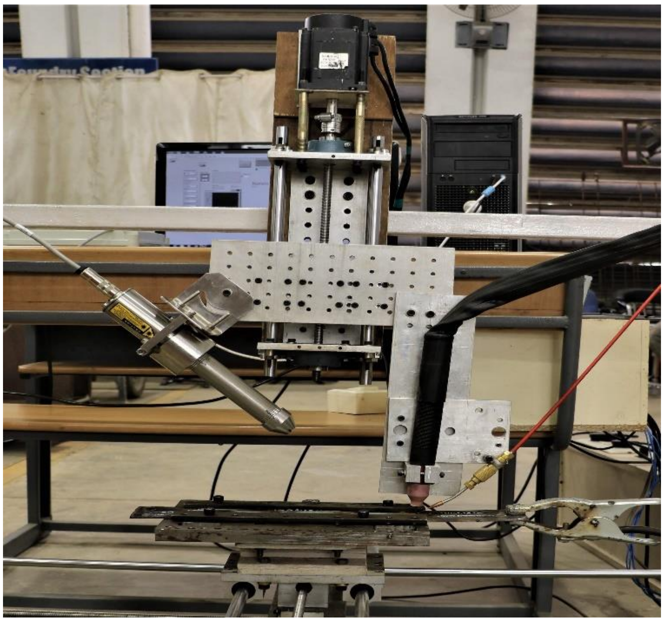

Figure 42: Experimental Arrangement For Deposition Of Single Bead Temperature Control

The temperature-dependent feedback control for the single bead deposition was introduced to control the deposition current (power) for obtaining the desired bead temperature, namely 1200°C, 1300°C and 1400°C for each deposition speed. Figure 43 shows the recorded controlled temperature during the deposition.

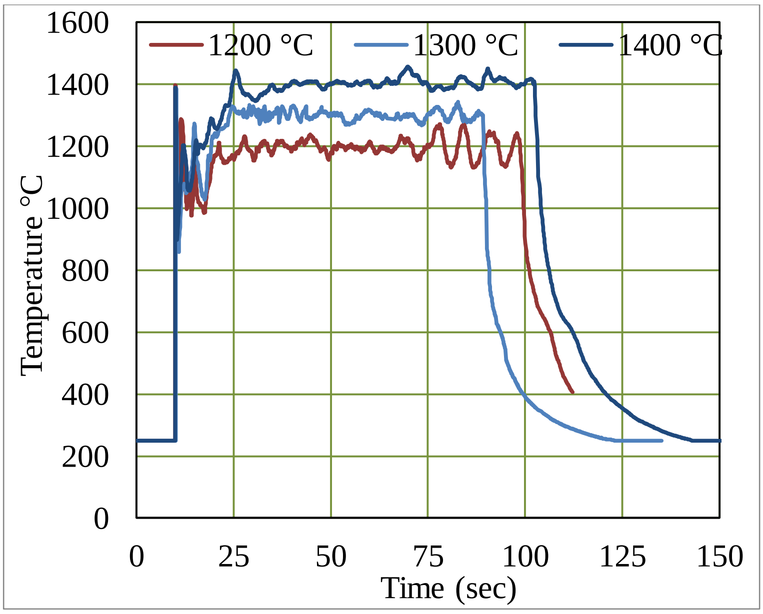

(a) Travel speed 150 mm/min

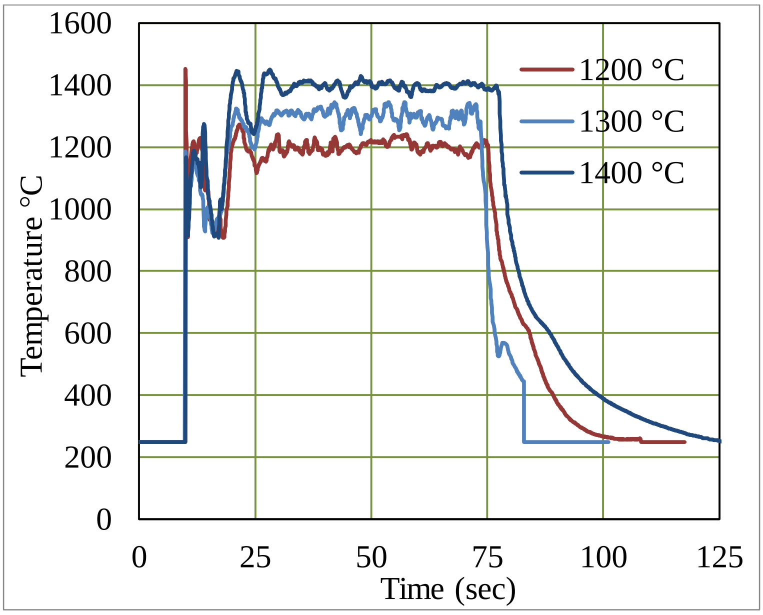

(b) Travel speed 200 mm/min

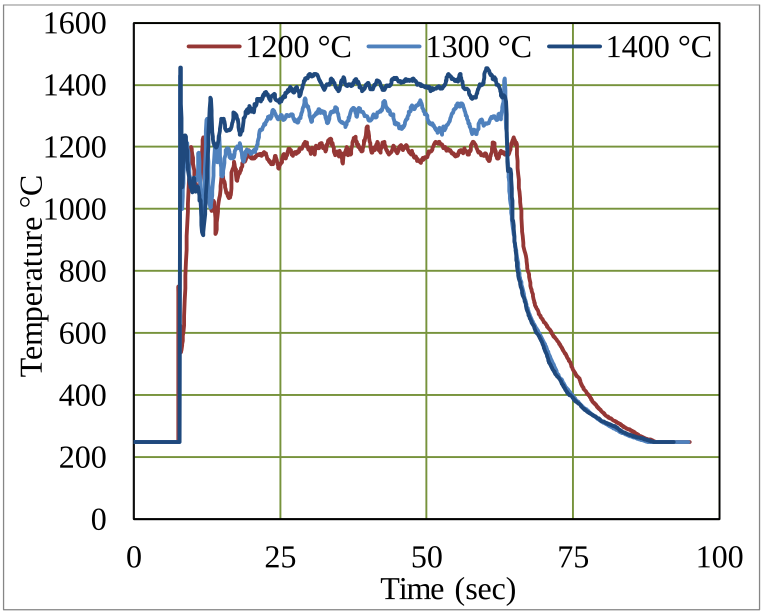

(c) Travel speed 250 mm/min

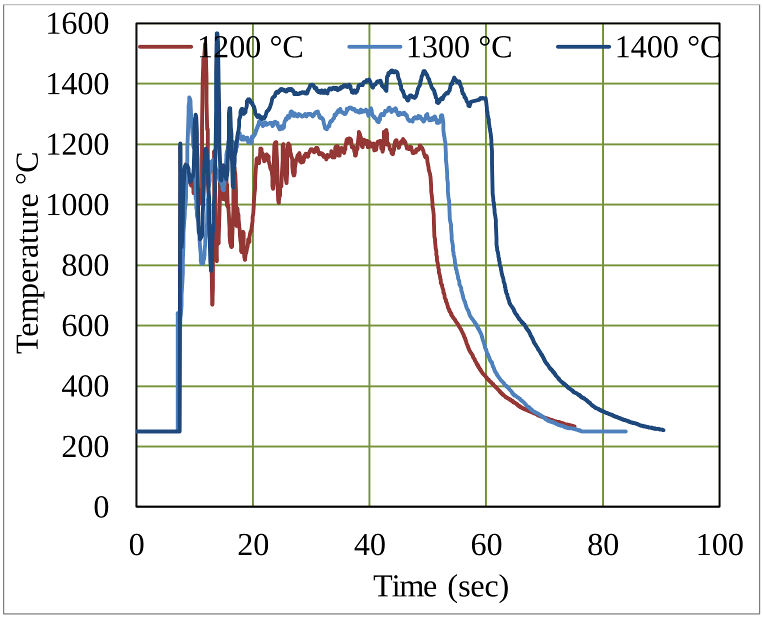

(d) Travel speed 300 mm/min

Figure 43: Feedback Temperature Control For The Moving Heat Source With Deposition At Different Travel Speed And Temperature (A) Travel Speed 150 Mm/Min (B) Travel Speed 200 Mm/Min (C) Travel Speed 250 Mm/Min (D) Travel Speed 300 Mm/Min

The experiments were also extended to control the temperature within a single track deposition. Figure 44 shows the single track feedback temperature control for both increasing trends (1200°C to 1400°C) and the decreasing trend (1400°C to 1200°C).

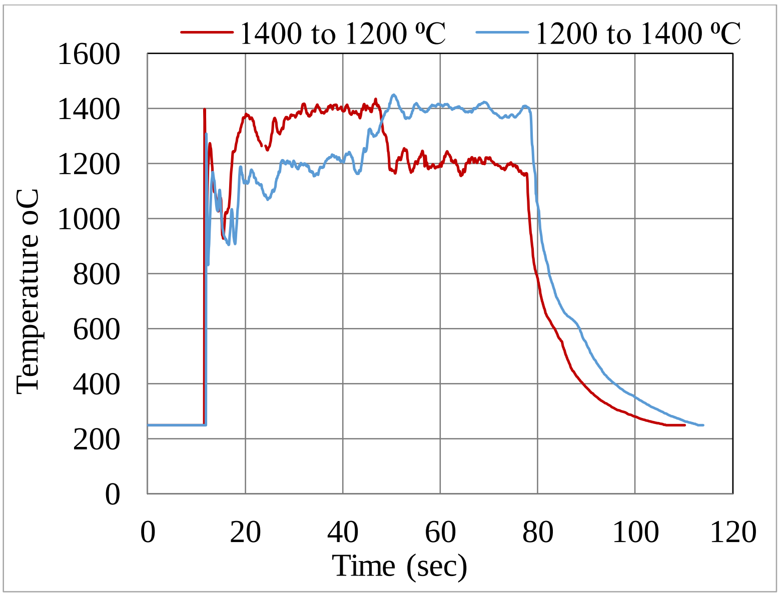

Figure 44: Single Track Deposition, Multiple Temperature Control At 150 Mm/Min Deposition Speed

It was observed that in all cases the bead temperature remains within the setpoint temperature. In all four cases, the calculated standard deviation in controlled temperature was found to be within ±25°C. This error was marginally higher than the previous cases. Also, the temperature was observed taking a relatively long time to get stabilised (20–25 sec). However, it includes the time required for any particular deposited point to reach the measurement point. This required time varies in the range of 2.4–4.8 sec depending on the deposition speed. During this time the pyrometer receives radiation only from the conducted heat as it was placed behind the arc. It could also be the reason for high fluctuation in measured temperature at the beginning. The bead deposition is considered to be a dynamic process, which involves heating, melting and again solidification of the material. These transition from liquid to solid-state and, further solid-solidification cooling leads to variation in surface emissivity [10]. This variation becomes significant when the cooling occurs at a fast rate, e.g. in the present study (~20 sec to reach a temperature of ~250°C), Figure 43. It would lead to scattered temperature data. The PID uses this data for the calculation of reference voltage. Hence, a long time would be required for PID to respond and find the optimum reference voltage, which eventually would become scattered. Since the utilised TIG power source could not be able to cope up with a very small change in current (resolution 1 Amp), the power would remain constant. Hence, the bead temperature would remain in its trend (either increasing or decreasing) for a longer duration, resulting in a marginal increase in error. The table shows the top view of beads deposited at 1200°C, 1300°C and 1400°C.

Table 3: bead geometry with respect to temperature

Controlled Temperature	Top view of deposited beads
1200°C 1300°C 1400°C	
1200-1400°C	

The top view shows the variation in bead size at different temperature with particular deposition speed. Also, a single bead is deposited at two different temperature (1200°C and 1400°C) and the geometry of bead changes.

Chapter 5 Conclusions and future scope

This chapter provides the conclusion of the research work done in the present research on temperature monitoring validation, TIG welding automation and control, online temperature and monitoring for stationary, moving and moving with the deposition heat source. Further, the future aspects of the research are discussed.

5.1 Conclusion

The objective of the present investigation was to in-situ monitor and controlled the generated temperature during TIG application. It is necessary to automate the TIG welding power source for programmable control to attain this objective.

- It was observed that the use of a ratio pyrometer would be an appropriate selection for the temperature monitoring as it has a little error in measurement.
- The ratio pyrometer significantly minimises the effect of external factors such as external radiation, fumes or dirt and change in emissivity. It makes it very useful in on-floor manufacturing applications where precise control in the environment would not be possible as demonstrated in this study.
- The temperature measurement in single-channel pyrometer is emissivity dependent, but ratio pyrometer is independent of emissivity. This concept was utilised to find the emissivity of tungsten and graphite.
- The temperature vs emissivity graph for tungsten and graphite is plotted for validation of temperature monitoring technique.
- A control system was developed in-house to replace the foot pedal control of the TIG power source for the successful implementation of the programmable control.
- The output power, i.e. current of TIG welding varies linearly with the reference voltage given by DAQ.
- Any foot pedal operated TIG machine can be automated, and output power can be controlled by computer with the help of LabVIEW.

- The feedback controlling using digital potentiometer is inefficient for a dynamic process such as TIG welding.
- The developed in-situ temperature monitoring and feedback control system worked very well for a broad range of temperature control between 400°C to 1600°C.
- The developed system works very well when tested in different experimental conditions such as stationary heating source (TIG torch) while monitoring the temperature in-line and offset, moving heat source at a different speed and bead deposition for additive manufacturing application.
- The optimised PID constants were found to be 1.0, 0.04 - 0.08, and 0.0 for proportional, integral and derivative, respectively.
- The calculated standard deviation in controlled temperature was found to be in the range of ±16°C and ±06°C, respectively, for in-line and offset focused control.
- The calculated standard deviation in controlled temperature was found to be in the range of ±15°C for moving heat source.
- The calculated standard deviation in controlled temperature was found to be in the range of ±25°C for moving heat source with deposition.
- A single bead was deposited successfully at a controlled temperature between 1200°C to 1400°C at different deposition speeds. It was evident that the control of deposition temperature has a direct relationship with the geometrical and mechanical properties of the deposited bead.

Fig. 45 variation in width and height of bead at 1400°C, 1300°C and 1200°C

- It was observed that for stationary heating, the setpoint temperature could be attained in relatively less time as compared to the moving heat source.
- The variation in temperature about setpoint depends on the temperature acquiring rate, i.e. faster the acquiring rate, faster the controlling rate.
- The error in controlled temperature was found in between 0.3–1.67% (5–25°C) depending on the experiments, whereas the maximum error was realised for the dynamic (moving TIG torch) and bead deposition temperature control 1–2% (15–25°C).
- The developed system would also be equally useful for other TIG based applications such as surface hardening, cladding, surface melting, alloying, etc.

5.2 Future Scope

- The control system can be used to manufacture complex 3D parts with negligible defects on WAAM.
- The relation between deposition temperature and bead parameter needs to be established, which can be used directly for a particular bead deposition.
- The detailed characterisation will give an insight into the controlling process.
- The developed control system can be used in cladding process to control the thickness of the cladding layer.

References

[1] Calignano F, Manfredi D, Ambrosio EP, Biamino S, Lombardi M, Atzeni E, et al. Overview on additive manufacturing technologies. Proc IEEE 2017;105:593–612. https://doi.org/10.1109/JPROC.2016.2625098.

[2] Guo N, Leu MC. Additive manufacturing: Technology, applications and research needs. Front Mech Eng 2013;8:215–43. https://doi.org/10.1007/s11465-013-0248-8.

[3] Horst D, Duvoisin C, Vieira R. Additive Manufacturing at Industry 4.0: a Review. Int J Eng Tech Res 2018;8:3–8.

[4] Pan Z, Ding D, Wu B, Cuiuri D, Li H, Norrish J. Arc Welding Processes for Additive Manufacturing: A Review BT - Transactions on Intelligent Welding Manufacturing 2018:3–24. https://doi.org/10.1007/978-981-10-5355-9.

[5] Ding D, Pan Z, van Duin S, Li H, Shen C. Fabricating superior NiAl bronze components through wire arc additive manufacturing. Materials (Basel) 2016;9. https://doi.org/10.3390/ma9080652.

[6] Z F. Processes and Mechanisms of Welding Residual Stress and Distortion. Woodhead Publishing Limited, Aington; 2005.

[7] Ding D, Pan Z, Cuiuri D, Li H. Wire-feed additive manufacturing of metal components: technologies, developments and future interests. Int J Adv Manuf Technol 2015;81:465–81. https://doi.org/10.1007/s00170-015-7077-3.

[8] Ding D, Pan Z, Cuiuri D, Li H. A practical path planning methodology for wire and arc additive manufacturing of thin-walled structures. Robot Comput Integr Manuf 2015;34:8–19. https://doi.org/10.1016/j.rcim.2015.01.003.

[9] Wu B, Pan Z, Ding D, Cuiuri D, Li H, Xu J, et al. A review of the wire arc additive manufacturing of metals: properties, defects and quality improvement. J Manuf Process 2018;35:127–39. https://doi.org/10.1016/j.jmapro.2018.08.001.

[10] Tapia G, Elwany A. A Review on Process Monitoring and Control in Metal-Based Additive Manufacturing. J Manuf Sci Eng Trans ASME 2014;136. https://doi.org/10.1115/1.4028540.

[11] Epsilon M. Basics of non contact temperature measurement n.d.:20. https://www.micro-epsilon.in/download/products/dat--infrared-basics--en.pdf.

[12] Williams SW, Martina F, Addison AC, Ding J, Pardal G, Colegrove P. Wire + Arc additive manufacturing. Mater Sci Technol (United Kingdom) 2016;32:641–7. https://doi.org/10.1179/1743284715Y.0000000073.

[13] Herzog D, Seyda V, Wycisk E, Emmelmann C. Additive manufacturing of metals. Acta Mater 2016;117:371–92.

https://doi.org/10.1016/j.actamat.2016.07.019.

[14] Karpagaraj A, Siva shanmugam N, Sankaranarayanasamy K. Some studies on mechanical properties and microstructural characterisation of automated TIG welding of thin commercially pure titanium sheets. Mater Sci Eng A 2015;640:180–9. https://doi.org/10.1016/j.msea.2015.05.056.

[15] Norman AF, Drazhner V, Prangnell PB. Effect of welding parameters on the solidification microstructure of autogenous TIG welds in an Al-Cu-Mg-Mn alloy. Mater Sci Eng A 1999;259:53–64. https://doi.org/10.1016/S0921-5093(98)00873-9.

[16] Mirshekari GR, Tavakoli E, Atapour M, Sadeghian B. Microstructure and corrosion behavior of multipass gas tungsten arc welded 304L stainless steel. Mater Des 2014;55:905–11. https://doi.org/10.1016/j.matdes.2013.10.064.

[17] Lv SX, Jing XJ, Huang YX, Xu YQ, Zheng CQ, Yang SQ. Investigation on TIG arc welding-brazing of Ti/Al dissimilar alloys with Al based fillers. Sci Technol Weld Join 2012;17:519–24. https://doi.org/10.1179/1362171812Y.0000000041.

[18] Nandagopal K, Kailasanathan C. Analysis of mechanical properties and optimisation of gas tungsten Arc welding (GTAW) parameters on dissimilar metal titanium (6Al-4V) and aluminium 7075 by Taguchi and ANOVA techniques. J Alloys Compd 2016;682:503–16. https://doi.org/10.1016/j.jallcom.2016.05.006.

[19] Kumar R, Ghosh PK, Kumar S. Thermal and metallurgical characteristics of surface modification of AISI 8620 steel produced by TIG arcing process. J Mater Process Technol 2017;240:420–31. https://doi.org/10.1016/j.jmatprotec.2016.10.020.

[20] Kumar S, Ghosh PK, Kumar R. Surface modification of AISI 4340 steel by multi-pass TIG arcing process. J Mater Process Technol 2017;249:394–406. https://doi.org/10.1016/j.jmatprotec.2017.06.035.

[21] Lin CM, Chang CM, Chen JH, Hsieh CC, Wu W. Microstructure and wear characteristics of high-carbon Cr-based alloy claddings formed by gas tungsten arc welding (GTAW). Surf Coatings Technol 2010;205:2590–6. https://doi.org/10.1016/j.surfcoat.2010.10.004.

[22] Advanced energy. No Title n.d. https://www.advancedenergy.com/globalassets/resources-root/manuals/en-op-igar-6-advanced-manual.pdf.

[23] Lv SX, Xu ZW, Wang HT, Yang SQ. Investigation on TIG cladding of copper alloy on steel plate. Sci Technol Weld Join 2008;13:10–6. https://doi.org/10.1179/174329307X249414.

[24] Sahoo CK, Masanta M. Microstructure and mechanical properties of TiC-Ni coating on AISI304 steel produced by TIG cladding process. J Mater Process Technol 2017;240:126–37. https://doi.org/10.1016/j.jmatprotec.2016.09.018.

[25] Amirsadeghi A, Sohi MH. Comparison of the influence of molybdenum and chromium TIG surface alloying on the microstructure, hardness and wear resistance of ADI. J Mater Process Technol 2008;201:673–7. https://doi.org/10.1016/j.jmatprotec.2007.11.157.

[26] Ulutan M, Yildirim MM, Buytoz S, Çelik ON. Microstructure and wear behavior of TIG surface-alloyed AISI 4140 steel. Tribol Trans 2011;54:67–79. https://doi.org/10.1080/10402004.2010.519859.

[27] Karamiş MB, Yildizli K. Surface modification of nodular cast iron: A comparative study on graphite elimination. Mater Sci Eng A 2010;527:5225–9. https://doi.org/10.1016/j.msea.2010.04.067.

[28] Orłowicz AW, Trytek A, Korzeniowski M, Kupiec B. Surface hardening of nodular cast iron by GTAW remelting. Arch Foundry Eng 2018;18:53–8. https://doi.org/10.24425/123601.

[29] Bi G, Gasser A, Wissenbach K, Drenker A, Poprawe R. Identification and qualification of temperature signal for monitoring and control in laser cladding. Opt Lasers Eng 2006;44:1348–59. https://doi.org/10.1016/j.optlaseng.2006.01.009.

[30] Müller B, Renz U. Development of a fast fiber-optic two-color pyrometer for the temperature measurement of surfaces with varying emissivities. Rev Sci Instrum 2001;72:3366–74. https://doi.org/10.1063/1.1384448.

[31] Forsythe WE, Adams EQ. Radiating Characteristics of Tungsten and Tungsten Lamps A Correction. J Opt Soc Am 1945;35:306. https://doi.org/10.1364/josa.35.000306.

[32] True THE. the True Temperature Scale of Tungsten and Its n.d.

[33] Verret DP, Ramanathan KG. Total Hemispherical Emissivity of Tungsten. J Opt Soc Am 1978;68:1167–72. https://doi.org/10.1364/JOSA.68.001167.

[34] Radiation S, Zohuri B. Blackbody Radiation Cryogenic Technologies 2018.

[35] Verret DP, Ramanathan KG. Total hemispherical emissivity of tungsten. J Opt Soc Am 1978;68:1167. https://doi.org/10.1364/josa.68.001167.

[36] Wang H, Chen D, Wang G, Long Y, Luo J, Liu L, et al. Measurement technology for material emissivity under high temperature dynamic heating conditions. Meas J Int Meas Confed 2013;46:4023–31. https://doi.org/10.1016/j.measurement.2013.07.041.

[37] Thorlabs n.d. https://www.thorlabs.com/thorproduct.cfm?partnumber=NENIR501B.

[38] IMPAC Pyrometer IGA 6/23 Advanced manual n.d. https://www.lumasenseinc.com/uploads/Products/Temperature_Measurement/Infrared_Thermometers/IMPAC_Pyrometers/Series_6/pdf/EN-IMPAC-Pyrometer-IGA-6-23-Advanced_Manual.pdf.

[39] NPTEL. arc welding power source 2 2013.

https://nptel.ac.in/courses/112/107/112107090/.